國立交通大學
顯示科技研究所

碩士論文

低溫鈍化技術於多功能薄膜之研究與應用

Application of low temperature passivation for muti-funtional thin film

研究生：鄭逸立
指導教授：劉柏村 博士

中華民國 九十七 年 六 月

低溫鈍化技術於多功能薄膜之研究與應用

Application of low temperature passivation for muti-funtional thin film

研究生：鄭逸立　　Student：Yi-Li Cheng

指導教授：劉柏村　博士　　Advisor：Dr. Po-Tsun Liu

國立交通大學
顯示科技研究所
碩士論文

A Thesis
Submitted to Department of Photonics and Display Institute
College of Electrical and Computer Engineering
National Chiao Tung University
in Partial Fulfillment of the Requirements
for the Degree of
Master
in
Photonics
June 2008
Hsinchu, Taiwan, Republic of China

中華民國九十七年六月

低溫鈍化技術於多功能薄膜之研究與應用

研究生：鄭逸立　　　　　　指導教授：劉柏村　博士

國立交通大學

光電工程學系 顯示科技研究所

摘要

在此論文裡，我們研究了介電常數材料在超臨界二氧化碳流體混合水的熱處理下其電性的改變。首先，在室溫下，利用電子束蒸渡系統成長極薄的氧化矽薄膜，厚度約為 7 奈米，為了取代傳統的高溫退火製程，能在未來於玻璃基本上運用。使用了溫度約 150°C 超臨界流體混合水的技術，為了驗證超臨界流體混合水能有效的使水分子進入到氧化矽，進而減少薄膜的缺陷密度，我們經由紅外線光譜儀、熱脫附常壓游離質譜儀與 X 射線光電子能譜來做材料分析，結果均顯示於氧化矽薄膜內氧的含量增加，而厚度為 7 奈米氧化矽薄膜在閘極電壓 3 伏特的操作下，其單位面積漏電流約為 2×10^{-7} A/cm^2，並且得到較高的崩潰電壓，崩潰電壓約為 6 伏特，傳導機制亦由原本未經過處理的量子穿隧效應轉換為熱放射效應，以上主要的原因是由於氧化矽薄膜的缺陷密度減少。

除此之外，我們發現在超臨界二氧化碳流體混合水處理過後的薄膜擁有非揮發性電阻式記憶體的特性。並且量測了其儲存的時間，可靠度，提出了相關的物理模型去解釋其儲存的成因。藉由薄膜內部處理過後剩餘的缺陷，施加足夠的偏壓下，使其缺陷內部電子發生局部穿隧的情形，進而改變能帶。產生了電阻的改變，達到記憶體的特性。

由這些結果均顯示，藉由超臨界流體混合水的技術，能減少薄膜的缺陷密度。並且也能在低溫下製造出記憶體。可預期的，若超臨界流體的特殊特性整合在介電常數材料、薄膜電晶體、太陽能電池與記憶體製程上，將具有其優勢。

Application of low temperature passivation for muti-funtional thin film

Student：Yi-Li Cheng　　Advisor：Dr. Po-Tsun Liu

Department of Photonics and Display Institute
National Chiao Tung University

Abstract

In this study, supercritical fluids (SCF) technology is employed originally to effectively improve the properties of low-temperature-deposited silicon oxide dielectric films. In this work, 7 nm ultra-thin Silicon Oxide (SiO_x) films are fabricated by e-gun method at room temperature, and replacing the conventional high temperature annealing with supercritical fluids treatment at 150 °C. The supercritical fluids act a transporter to deliver H_2O molecule into the SiO_x films for repairing defect states. After this proposed process, the absorption peaks of Si-O bonding apparently raise and the quantity of oxygen in SiO_x film increases from FTIR and TDS measurement, individually. The leakage current density of 7 nm SiO_x film is cut down to 2×10^{-7} A/cm^2 at $|Vg| = 3$ V, and the conduction mechanism is transferred from quantum tunneling to thermal emission because of the significantly reducing the defects in the SiO_x film. Moreover, the higher breakdown voltage is obtained, reaching $|Vg| = 6$ V.

Additionally, the RRAM characteristics was found in SiO_x film treated by supercritical fluid,and retention,endurance were measured.when less trap was in treated film,the bias was applied enough on film,that made tunning effect happened inside.The resistence changed was by binding energy .

誌 謝

這兩年以來受到許多人幫助及教導。首先要感謝我的論文指導教授劉柏村博士，帶我知道研究的領域及待人接物的處理。以及感謝中山物研教授張鼎張博士對實驗的方向及內容有許多的協助，誠摯的感謝老師的幫助。以及諸位口試委員得指導讓實驗的內容更為完善。

並且感謝蔡志宗學長在超臨界流體技術中帶領我一窺奧秘, 以及論文中多所協助及指導。此外楊柏宇學長、周誼明學長、高逸侑學長對實驗機台及內容的教導也是由衷的感謝。還有要感謝陳緯仁學長、吳興華學長、鄒一德學長、陳世青學長、葉炳宏學長、曹書瑋學長、馮立偉學長、弘偉學長，盧皓彥學長感謝學長們平日對我的照顧以及研究上的建議。也要感謝實驗室一起工作的同學－郭豫杰、竹立煒、林威廷、陳巍方、王超駿、張繼聖、蔡尚祐、陳思維…等，以及學弟－王信淵、張耿維…等，因為有了你們在這兩年的過程中多了許多歡樂。還有NDL及奈米中心許多的工程人員在這兩年的過程中感謝諸位的協助，尤其奈米中心的林先生感謝你在製程上許多建議及協助。

最後感謝我的父母親，鄭金漳先生以及呂秋菊女士。如果沒有您們在我的背後提供需多協助及幫忙，將不能心無旁誤的把心力用在實驗上面。

鄭逸立 2008 年 6 月

Contents

Chapter 1 Introduction

Chapter 2 Application of Supercritical Fluid Technology on Silicon-Oxide Dielectric Thin Film

Chapter 3 Application of Supercritical Fluid Technology on Resisitive Random Access Memory

References

Table Captions

Chapter 1

Chapter 2

Figure Captions

Chapter 1

Chaprer 2

Chapter 3

Chapter 1

Introduction

1.1 Supercritical Fluid Technology

Supercritical fluids are compounds above their critical temperatures and pressure, as shown in Fig 1-1 [1, 2]. The attractiveness of supercritical fluids for commercial applications is their unique combination of liquid-like and gas-like properties. The Table 1-1 shows critical temperature and pressure for some common fluids. CO_2-based supercritical fluids are particularly attractive because CO_2 is non-toxic, non-flammable, and inexpensive. Besides, its critical conditions are easily achievable with existing process equipment (31 °C, 1072 psi =72.8 atm).

Figure 1-2 shows the density-pressure-temperature surface for pure CO_2. It can be discovered that relatively small changes in temperature or pressure near the critical point, resulting in large changes in density. Table 1-2 shows the comparison of several physical properties of typical liquid, vapor, and supercritical fluid state for CO_2. It could be seen that supercritical CO_2 ($SCCO_2$) fluids possesses liquid-like density, so that $SCCO_2$ fluids are analogous with light hydrocarbon to dissolve most solutes and own exceptional transport capability [3, 4]. On the other hand, $SCCO_2$ fluids hold gas-like characteristic due to their viscosity and surface tension are extremely low, it allows $SCCO_2$ fluids to keep fine diffusion capability and enter the nano-scale pores or spaces without damage. These properties are the reasons for $SCCO_2$ fluids to employ in many commercial applications, including the extraction of caffeine from coffee, fats from foods, and essential oils from plants for using in perfumes. Furthermore, in last years, many records are investigated with $SCCO_2$ fluids to apply in semiconductor fabrication, such as cleaning wafer and stripping photoresist, by means of its high mass transfer rates and infiltration capabilities [4-6].

1.2 General Background

1.2.1 Low temperature Oxide dielectric films

In the recent years, Low-temperature polycrystalline silicon (LTPS) thin-film transistors have been widely studied because of their potential applications in high-performance displays Together with improvements in display technology, the low-temperature polysilicon (LTPS) TFT LCD is expected to be one of the most promising displays for digital tools such as Liquid crystal display and PDA.

SiOx thin film is known to have excellent properties such as hardness, wear-resistance, anti-corrosion and also optical, dielectric properties, so it is widely applied as the gate dielectric of transistor and the tunneling oxide of non-volatile memory. [7-9] The total does radiation hardess of the gate insulator used in MOS devices is strogly determined by the details of the oxide growth and annealing process. The development of low cost, rugged plastic and glass displays could lead to a dramatic increase in both the variety and utility of military and consumer display products. the added feature of flexibility may lead to the creationof entirely new display markets. The primary advantages of plastic and glass substrates with respect to silicon are a reduction in theweight of the display, flexibility, and a reduction in display breakage, both during fabrication and use Additionally. A growing demand for new applications of thin film microelectronicsin portable lightweight systems has resulted in a need for reduced maximum processing temperatures during fabrication of integrated circuits. For example, in the flat panel display industry researchers are continually lowering processing temperatures required to form the polycrystalline Si films for thin film transistors (TFTs) to allow the use of lower cost substrates.

1.2.2 Nonvolatile resistive switching memory

Since the first observation of bistable resistance states in the 1960's, reversible and reproducible resistance switching phenomena caused by applied electric field have been investigated widely to be used as resistive random access memories (RRAM). Recently, numerous metal oxides and perovskite oxides including Nb2O5, TiO2, and Nb-doped SrTiO3 have been reported for RRAM applications. Nevertheless, there is only few studies mention the process of resistance memory at low temperature. The binary oxide MIM memory devices were discovered decades ago [10]. This device had not been a serious contender for large scale memory array application. After the publication of electric-pulse-induced reversible (EPIR) resistance non-volatile memory by Liu et al in 2000 the ternary MIM memory, which we referred as RRAM, devices have attracted considerable interest. Resisitive RAM (RRAM) development is generally based on using an electrical pulse to change the resistance across a thin film of either a simple binary metal oxide or a more complex perovskite oxide. It has been the focus for reearch at several device manufacturers and some startups because it promises high density, low cost and low power consumption, along with non-volatility. It has the classic profile of the much-sought-after universal memory that could combine the speed of SRAM with density of DRAM and the nonvolatility of flash memory.

1.3 Motivation

In recent years, many reports interests in the formation of SiO_x film at low temperature (≦ 200 °C) for fabricating electron devices on flexible plastic substrates.[11-13] Among various deposition methods, the physical vapor deposition (PVD) is favorable as a result of the advantages of simple process, low cost, and conformity with low-temperature fabrication. Nevertheless, a high temperature annealing or plasma treatment is generally taken as post-treatment to passivate the traps in PVD-deposited film for improving the dielectric characteristics. Due to the limit of glass transition temperatures (T_g), these high temperature post-treatments are unsuitable to plastic substrates,[6] and a low temperature treatment to passivate traps is required.

the $SCCO_2$ fluid is proposed to fabricate the resistance memory at 150 °C, so it would be applicable to product RRAM on the substrates with low glass transition temperatures (T_g). The supercritical fluid technology is generally used for the impurity extraction, dehydration and drying of materials with a fine structure. It also had employed $SCCO_2$ fluid to deliver oxidant into metal oxide film for terminating electric defects by the gas-like and liquid-like properties. According to the mechanisms of bistable resistance states are possibly dominated by some kind of charge trap, the we would employ $SCCO_2$ technology to fabricate a resistance memory by varying the trap density in SiO_x film. The experimental works will focus on the effect of passivating traps by $SCCO_2$ treatment and investigate the influence of varying trap density on resistance switching phenomena.

Chapter 2

Application of Supercritical Fluid Technology on Silicon-Oxide Dielectric Thin Film

2.1 Fabrication of Silicon-Oxide and Experiment Process

The e-gun system was used to deposit SiO_x films on p-type (100) silicon wafer under 2×10^{-6} torr at room temperature, and the average thickness of SiO_x films measured by ellipsometer system is 5-7 nm. For enhancing the quality of these ultra-thin SiO_x films, three different post-treatments were applied individually. First method, labeled as "*H_2O vapor treatment*", is immersing the SiO_x film into a pure H_2O vapor ambience at 150 °C for 2 hrs, in a stainless steel chamber. Second method, labeled as *"3000 psi-$SCCO_2$ treatment"*, is placing the SiO_x film in supercritical fluid system at 150 °C for 2 hrs, where was full of 3000 psi-$SCCO_2$ fluids mixed with 8 vol.% ethyl alcohol and 2 vol.% pure H_2O. The ethyl alcohol acts surfactant between nonpolar $SCCO_2$ fluids and polar H_2O molecules to making the uniform distribution of H_2O molecules in $SCCO_2$ fluids, and the $SCCO_2$ fluids thereby could transport H_2O molecules efficiently into SiO_x layer to react with traps. In comparison with 3000 psi-$SCCO_2$ treatment, the third method is treating SiO_x film with 3000 psi pure $SCCO_2$ fluids but no co-solvent was added, and labeled as "*$SCCO_2$-only*". The supercritical fluid system is shown in Fig. 2-1.Afterward, the Al metal was thermally evaporated on the top surface of these treated SiO_x films and the backside of silicon wafer as electrodes to shape the metal insulator semiconductor (MIS) structure. The Fourier transformation infrared spectroscopy (FTIR) was applied to determine the evolution of chemical functional bonding after different treatment. The atomic content of SiO_x film was detected from Auger electron spectroscopy (AES) analysis, and the electrical behaviors of SiO_x film were measured by HP 4156-A semiconductor analyzer and

Agilent 4284A CV meter. The experiment processes of thin SiO_x film with various treatments are exhibited in Fig. 2-2.

2.2 Analysis of Material and Discussion

2.2.1 Fourier Trans-form Infrared Spectroscopy (FTIR) Analysis

The FTIR spectra of SiO_x films after different treatments are shown in Fig. 2-3, and the un-treated SiO_x film is taken as background. For $SCCO_2$-only treated SiO_x film, there is no IR absorption peak appears in the wavenumber of 400-1500 cm^{-1}, i.e. the $SCCO_2$ fluid wouldn't affect the functional structure of SiO_x. In the case of H_2O-vapor treated SiO_x film, however, vibration bands for Si–O stretching at 1080 cm^{-1}, Si=O stretching at 1230 cm^{-1}, Si–O rocking at 440 cm^{-1}, and S-H bending at 610 cm^{-1} increase clearly. [14]The raise of IR absorption peak indicates that the H_2O molecules could infiltrate into SiO_x film and modify the quality of SiO_x film during H_2O-vapor process. Because the main variation occurs in S-O bonding, it is believed that the H_2O molecule is operative oxidant to react with Si dangling bond, and this agrees with prior literatures. [15~16] The same IR absorption peaks are also observed for 3000-psi $SCCO_2$ treated SiO_x film, and the higher absorption peaks express that $SCCO_2$ fluid added with co-solvent (8 vol.% ethyl alcohol and 2 vol.% H_2O) is a more operative method than H_2O-vapor to enhance the quality of SiO_x films. Therefore, the $SCCO_2$ fluids mixed with co-solvent would completely infiltrate in into SiOx films as the pressure increasing in 3000psi, and the best improvement for SiOx films is achieved because of advancing the reaction probability between H_2O molecule and Si dangling bonds. , and the transporting mechanism for $SCCO_2$ fluids taking H_2O molecule into SiO_x film is shown in Fig. 2-4

2.2.2 Thermal Desorption System – Atmospheric Pressure Ionization Mass Spectrometer (TDS-APIMS) Analysis

The TDS measurement, as shown in the Fig. 2-5, was carried out upon heating these treated SiO_x films from 50 to 800 °C at a heating rate of 10 °C/min in vacuum (10^{-5} Pa.). In Fig. 2-5 (a), m/e (mass-to-charge ratio) = 18 peak that is attributed to H_2O was monitored to evaluate the content of residual moisture in SiO_x films. It is clearly found the same H_2O content is detected in the $SCCO_2$-col, H_2O-vapor and 3000 psi-$SCCO_2$-treated SiO_x film, certainly consistent with the FTIR observation. From Fig. 2-5 (b), m/e (mass-to- charge ratio) = 44 peak that is attributed to CO_2, the residual CO_2 in SiO_x is equal the same after 3000 psi-$SCCO_2$, H_2O-vapor and pure $SCCO_2$ treatment. This is result from $SCCO_2$-col, , H_2O-vapor and pure $SCCO_2$ treatment mean that no residual moisture and CO_2 in the SiO_x film. Therefore different Electrical Characteristics were not induced by residual moisture and CO_2.

2.2.3 X-ray Photoelectron Spectroscopy (XPS) Analysis

XPS involves measuring the photoelectron spectra obtained when a sample surface is irradiated with x-rays. The kinetic energy (peak position) of the photoelectrons can be written as

$$E_K = h\nu - E_B - \phi_s - q\phi$$

where $h\nu$ is the x-ray energy, E_B is the binding energy (the difference between the Fermi level and the energy level being measured), ϕ_s is the work function of the electron spectrometer, q is the electronic charge, and ϕ is the surface potential.

We have also performed XPS measurements using an Al Kα X-ray source (1486.6 eV photons) to determine the bonding environments of the Si and O atoms. the XPS spectra for Si 2p level that were calibrated from C 1s peak at 284.5 eV. Each spectrum was represented the result at different post-treatments, including $SCCO_2$-only,

H_2O vapor and 3000psi-$SCCO_2$ treatment. The first group labeled as pure $SCCO_2$ treatment, was designed as the control sample, and was only is treating SiO_x film with 3000 psi pure $SCCO_2$ fluids but no co-solvent was added,s. The second group labeled as H_2O vapor treatment, was immersed into a pure H_2O vapor ambience at 150 °C for 2 hrs in a pressure-proof stainless steel chamber with a volume of 30cm^3. The third group marked as 3000psi-$SCCO_2$ treatment, was placed in the supercritical fluid system at 150°C for 2 hrs, where was injected with 3000psi of $SCCO_2$ fluids mixed with 5 vol.% of ethyl alcohol and 5 vol.% of pure H_2O. As shown in Figure 2-6 , the Si2p peak, which have binding energies of 103.9 and 99 eV, respectively related to Si-O bonding and Si=Si in SiO_x. However, the binding energy of Si_{2p} peak shown in Figure 2-6 varied from 103.8 eV for pure $SCCO_2$ fluids sample to 104.1 eV for 3000psi-$SCCO_2$ treatment sample. The origins of binding energy shift (ΔBE) are suggested as a number of factors such as charge transfer effect, presence of electric field, environmental charge density, and hybridization. Among these, charge transfer is regarded as a dominant mechanism causing a binding energy shift. According to the charge transfer mechanism, removing an electron from the valence orbital generates the increment in core electron's potential and finally leads a chemical binding energy shift [17]. Therefore, it is considered that the Si_{2P}peaks shift originated from the enhanced charge transfer with different post-treatments, *i.e.*, the larger portion of Si atoms was fully oxidized with *3000psi-*$SCCO_2$ *treatment*. Figure 2-7 shows the O 1s core level peaks also demonstrated binding energy shift with changing of different post-treatments. Each peak can be split into two sub-peaks by Gaussian fitting which represent the O-Si bonding at ~533 eV [18,19]. The peak intensity of O-Si bond for different treatments is not the same, meaning that these post-treatments would make different influence on the thickness and quality of the interfacial SiO_x film. For the H_20 vapor SiO_x film, however, the peak intensity of Si-O bands raises apparently in comparison with the pure $SCCO_2$ fluids -treated SiO_x film. This is believed well that the H_2O vapor would permeate into SiO_x film and makes reaction with Si dangling bonds (i.e. traps) forming Si-O bands. [20~22]. These traps in the low-temperature deposited SiO_x film could be thereby passivated by H_2O vapor molecules. Furthermore, with $SCCO_2$ treatment, obvious increase in the intensity of Si-O bonding is observed in the XPS. It indicates that the best transport efficiency of H_2O molecules into SiO_x film is achieved by the $SCCO_2$ fluids, potentially modifying the dielectric properties of SiO_x film, and the transporting mechanism for $SCCO_2$ fluids taking H_2O molecule into SiO_x film is shown in Fig. 2-4. Summary of binding energies for SiO_x films are shown in Table 2-1 and Table 2-2.

2.2.4 Auger Electron Spectroscopy (AES) Analysis

In order to analyze the composition of the silicon oxide film after various post-treatments, including pure $SCCO_2$ fluids, H_2O vapor and 3000 psi-$SCCO_2$ treatment, we performed the Auger electron spectroscopy analysis. The first group labeled as pure $SCCO_2$ fluids treatment, was designed as the control sample, and was only treated in pure $SCCO_2$ fluid at 150 °C for 2 hrs. The second group labeled as H_2O vapor treatment, was immersed into a pure H_2O vapor ambience at 150 °C for 2 hrs in a pressure-proof stainless steel chamber with a volume of $30cm^3$. The third group marked as 3000psi-$SCCO_2$ treatment, was placed in the supercritical fluid system at 150°C for 2 hrs, where was injected with 3000psi of $SCCO_2$ fluids mixed with 5 vol.% of propyl alcohol and 5 vol.% of pure H_2O. The ethyl alcohol plays a role of surfactant between nopolar-$SCCO_2$ fluids and polar-H_2O molecules, so that the H_2O molecule uniformly distributes in $SCCO_2$ fluids and be delivered into the SiO_x film for passivating defects. As shown in Figure 2-8, the pure $SCCO_2$ fluids-treated and H_2O vapor-treated films has oxygen composition lower than that of the silicon oxide film after 3000 psi-$SCCO_2$ treatment. The ethyl alcohol plays a role of surfactant between nopolar-$SCCO_2$ fluids and polar-H_2O molecules, so that the H_2O molecule uniformly distributes in $SCCO_2$ fluids and be delivered into the SiO_x film for passivating defects.

2.3 Analysis of Electrical Characteristics and Discussion

2.3.1 The current density-electric field (*J-E*) characteristics

The plot of leakage current density of SiO_x films versus electric field is displayed in Fig2-10. to realize the influence of different treatment on dielectric characteristics. Among various post-treatments, the pure $SCCO_2$ fluids SiO_x film exhibits the most serious leakage current, inferentially due to its poor dielectric characteristics with numerous traps inside the SiO_x film. The improvement of electrical characteristics is observed by using H_2O vapor process, however, a high leakage current density still appears at larger applied voltages. It could be inferred reasonably dependent on the defect passivation efficiency. The most indicating that H_2O vapor can passivate the traps (or defects) and alter dielectric properties of the low-temperature-deposited SiO_x film. After H_2O vapor treatment, effective improvement of electrical characteristic is obtained by the 3000 psi-$SCCO_2$ treatment, exhibiting the lowest leakage current density among all samples. Low leakage current density (less than 10^{-7} A/cm^2). is kept constantly, even biased at an electric field of 3 MV/cm. The electrical performance agrees with FTIR analysis, in which 3000 psi-$SCCO_2$ treatment modified SiO_x dielectrics even effectively.

2.3.2 Conduction Mechanism

There may be different conduction mechanisms in the insulator thin film, including Schottky-Richardson emission [23], Frenkel-Poole emission [23,24], Fowler-Nordheim tunneling [23,24], and trap assisted tunneling [25,26] illustrated in Fig 2-9. The Schottky-Richardson emission generated by the thermionic effect is caused by the electron transport across the potential energy barrier via field-assisted lowering at a metal-insulator interface. The leakage current governed by the Schottky-Richardson emission is as following:

$$J_{SR} = A^{*}T^{2}\, exp\left(\beta_{SR}E^{1/2} - \phi_{SR}/k_{B}T\right)$$

where $\beta_{SR} = \left(q^3 / 4\pi\varepsilon_0\varepsilon\right)^{1/2}$, q is the electronic charge, A^* is the effective Richardson constant, ϕ_{SR} is the contact potential barrier, E is the applied electric field, ε_0 is the permittivity in vacuum, ε is the high frequency relative dielectric constant, T is the absolute temperature, and k_B is the Boltzmann constant. We can find the slope of the leakage current equation.

$$\ln J_{SR} = \beta_{SR} E^{1/2} / k_B T + \left[\ln\left(\mathrm{A}^* \mathrm{T}^2\right) - \phi_{SR} / k_B T\right]$$

$$Solpe = \beta_{SR} / k_B T$$

The Frenkel-Poole emission is due to field-enhanced thermal excitation of trapped electrons in the insulator into the conduction band. The leakage current equation is:

$$J_{FP} = J_0 \, exp\left(\beta_{FP} E^{1/2} - \phi_{FP} / k_B T\right)$$

where $J_0 = \sigma_0 E$ is the low-field current density, σ_0 is the low-field conductivity, $\beta_{FP} = \left(q^3 / \pi\varepsilon_0\varepsilon\right)^{1/2}$, q is the electronic charge, ϕ_{FP} is the contact potential barrier, E is the applied electric field, ε_0 is the permittivity in vacuum, ε is the high frequency relative dielectric constant, T is the absolute temperature, and k_B is the Boltzmann constant. We can find the slope of the leakage current equation.

$$ln\, J_{FP} = \beta_{FP} E^{1/2} / k_B T + \left[ln\left(J_0\right) - \phi_{FP} / k_B T\right]$$

$$Solpe = \beta_{FP} / k_B T$$

The Fowler-Nordheim tunneling is the flow of electrons through a triangular potential barrier. Tunneling is a quantum mechanical process similar to throwing a ball against a wall often results that the ball goes through the wall without damaging the wall or the ball. It also loses no energy during the tunnel event. The probability of this event happening, however, is extremely low, but an electron incident on a barrier typically several nm thick has a high probability of transmission. The Fowler-Nordheim tunneling current I_{FN} is given by the expression [27]:

$$I_{FN} = A_G A_{FN} \varepsilon_{ox}^2 \, exp\left(-B_{FN}/\varepsilon_{ox}\right)$$

where the A_G is the gate area, ε_{ox} is the oxide electric field, and A_{FN} and B_{FN} are usually considered to be constant. A_{FN} and B_{FN} are given as the following:

$$A_{FN} = q^3\left(m/m_{ox}\right)/8\pi\, h\Phi_B = 1.54\times 10^{-6}\left(m/m_{ox}\right)/\Phi_B$$

$$B_{FN} = 8\pi\left(2m_{ox}\Phi_B^3\right)^{1/2}/3eh = 6.83\times 10^7\left[\left(m/m_{ox}\right)\Phi_B^3\right]^{1/2}$$

where m_{ox} is the effective electron mass in the oxide, m is the free electron mass, q is the electronic charge, and Φ_B is the barrier height at the silicon-oxide interface given in units of eV in the expression for B_{FN}. Φ_B is actually an effective barrier height that take into account barrier height lowering and quantization of electrons at the semiconductor surface. Rearranging I_{FN} formula gives by:

$$ln\left(I_{FN}/A_G\varepsilon_{ox}^2\right) = ln\left(J_{FN}/\varepsilon_{ox}^2\right) = ln\left(A_{FN}\right) - B_{FN}/\varepsilon_{ox}$$

A plot of $ln\left(J_{FN}/\varepsilon_{ox}^2\right)$ versus $\left(1/\varepsilon_{ox}\right)$ should be a straight line if the conduction through the oxide is pure Fowler-Nordheim conduction [27].

In the trap assisted tunneling model, it is assumed that electrons first tunnel through the SiO_X interfacial layer (direct-tunneling). Then, electrons tunnel through traps located below the conduction band of the high-k thin film and leak to substrate finally [25]. The equation of leakage current density is [26]:

$$J = \alpha/E_{ox} \, exp\left(-\beta/E_{ox}\right)$$

From the equations as shown above, leakage current behaviors of insulate films can be investigated further on the leakage current density J electric field E characteristics such as J vs. $E^{1/2}$ plots.

The plot of the nature log of leakage current density versus the square root of the applied electric field was observed. It is found that the leakage current density is linearly related to square root of the applied electric field. The linear variations of the current correspond either to Schottky-Richardson emission or to Frenkel-Poole conduction mechanism. For trap states with coulomb potentials, the expression is virtually identical to that of the Schottky-Richardson emission. The barrier height, however, is the depth of the trap potential well, and the quantity β_{FP} is larger than in the case of Schottky-Richardson emission by a factor of 2.

Leakage conduction mechanism is also investigated to support the comments on the electrical improvement of SiO_x film. Fig. 2-11(a) plots ln (J/E) versus reciprocal of electric field variation for the pure $SCCO_2$ fluids treated SiO_x film, and a schematic energy band diagram accounting for leakage transport mechanism shown in the inset. A good linear fitting explains Fowler-Nordheim (F-N) tunneling [28] occurs in the electric fields higher than 1.2 MV/cm. Also, it is consistent with the electrical behavior of pure $SCCO_2$ fluids treated SiO_x film in Fig. 2-10 that leakage current density sharply increases, while gate bias voltage larger than 1.2 MV/cm. This could be attributed to the trap-assisted tunneling due to numerous traps inside the 150°C- pure $SCCO_2$ fluids treated SiO_x film [29]. For the 3000 psi-$SCCO_2$ treated SiO_x film, a plot of leakage current density versus the square root of the applied field ($E^{1/2}$) gives a good representation of the leakage behavior at high electric fields, as shown in Fig. 2-11(b). The leakage current density of the 3000 psi-$SCCO_2$ treated SiO_x is linearly related to the square root of the applied electric field, demonstrating Schottky-Richardson emission transport mechanism [30]. The Schottky-type conduction can be verified by comparing the theoretical value of $\beta_{SR} = \left(q^3/4\pi\varepsilon_0\varepsilon\right)^{1/2}$ with the calculated one obtained from the slope of the experimental curve ln J versus $E^{1/2}$ [31], where q is the electronic charge, ε_0 the dielectric constant of free space, ε is the high frequency relative dielectric constant. The Schottky emission generated by the thermionic effect is caused by electron transport across the potential energy barrier via field-assisted lowering at a metal-insulator interface, shown in the insert of Fig. 2-11(b), and independent of traps. From the slope of ln J versus $E^{1/2}$, the calculated value of relative dielectric constant (ε) is 3.5, and which is close to the determined value of 3.8 in capacitance-voltage (C-V) measurement (referring to table 2-3). This also proves, for 3000spi-$SCCO_2$ treated SiO_x film, the conduction mechanism is really Schottky emission, but not trap-dependent Poole-Frenkel emission [31]. Additionally, the evolution of conduction mechanisms from trap-assisted tunneling to Schottky emission can confirm these defects inside low-temperature-deposited SiO_x film is minimized effectively by implementing the proposed $SCCO_2$ technology. The leakage current densities of SiO_x films after different treatments are shown as a function of applied positive gate bias voltage in Fig. 2-12, and the lower leakage current still could be acquired after 3000 psi-$SCCO_2$ and H_2O vapor treatment, especially treated with $SCCO_2$ fluids. This could be attributed to the influence of traps in the interface between parasitical SiO_x and Si wafer. Generally, in positive gate bias, the sources of electron are (1) the interface states, (2) defects in depletion region, (3) back electrode of substrate, [33] and the later two source are negligible due to the p-type signal-crystal Si wafer is used in this work. For pure $SCCO_2$ fluids treated SiO_x film, the great quantity of interface states still exist which generate electron-hole pair and lead to higher leakage current, as described in the inset of Fig. 2-12 After 3000 psi-$SCCO_2$ treatment, the interface states were deactivated, hence the leakage current is reduced. The reduction of interface states would be proved in capacitance-voltage measurement. [36]

2.3.3 The capacitance-voltage (*C-V*) characteristics

The capacitance-voltage (*C-V*) characteristics are also generally used to judge the quality of dielectric films. Figure 2-13 shows capacitance-voltage characteristics of SiO_x films after different treatment, measuring at 1M Hz with gate bias swing from negative voltage to positive voltage (forward) and from positive voltage to negative voltage (reverse). The slope of C-V curve in transient region, i.e. from C_{max} to C_{min}, is relative to the interface states, for example, the sharp slope indicates fewer defects exist in the interface between SiO_x and Si wafer. In Fig. 2-13, the pure $SCCO_2$ fluids -treated SiO_x film presents the worst C-V curve and lower capacitance. This expresses the number of interface states exist and lead to the smooth C-V curve. Additionally, the lower dielectric constant, as shown in table 2-3, could be referred to the influence of defects in SiO_x film. With H_2O vapor treatment, the sharper C-V curve and higher capacitance are obtained, and it could be attributed to the reduction of defects in SiO_x film and the interface. Furthermore, the best improvement is achieved by 3000 psi-$SCCO_2$ treatment. This exhibits that the $SCCO_2$ treatment possesses excellent ability to passivate the defects, including Si dangling bonds and interface states.

Besides, from Fig. 2-13, the shift of C-V curve under forward and reverse swing is also appears in pure $SCCO_2$ fluids and H_2O vapor-treated SiO_x films. It is resulted from the trapped carrier in defects of SiO_x films, and that is not expected for gate insulator of transistors. Under negative gate bias, the electric inject from Al gate into SiO_x films and trapped by defects, leading to the larger gate bias is required for inducing electron-inversion layer. For describing clear, These results conform to the tendency in current-voltage characteristics and again verify that the $SCCO_2$ technology could effectively deactivate defects in SiO_x films.The main reason could be referred to the positively charged Si dangling bonds are passivated as a matter of fact, upon reducing the oxide thickness, it is difficult to calculate the density of interface states by using the high-low frequency method because of the substantially increased gate leakage current.

2.3.4 Breakdown voltage measurement and gate bias stress

Figure 2-14 show the breakdown characteristic curves of SiO_x films after various treatments at negative gate bias region, individually. The breakdown voltage is mainly relative to the qualities of dielectric films and the density of defects in the dielectric films. A large number of traps lead to the trap-assisted tunneling early occurs and a high leakage current appears at small electric field, such that the lower breakdown voltages of dielectric films comes up. In Fig. 2-15, whether at negative gate bias, the pure $SCCO_2$ fluids -treated SiO_x film presents the worst performance in breakdown voltage because of the high density of defects, and the improvements of breakdown voltage are gradually achieved via H_2O vapor and 3000 psi-$SCCO_2$ treatment. This result exhibits clearly that the density of defects in SiO_x films are effectively reduced, and the breakdown voltage of 5~7nm SiO_x film thereby could be substantially ameliorated from 1 V to 10 V at negative gate bias. It also indicates that the $SCCO_2$ fluids technology is greatly useful to enhance the low-temperature deposited SiO_x films by passivating defects, and allows the treated SiO_x film holding good reliability as the gate dielectric.

Another important property of dielectric films is the reliability under gate bias stress. Due to the gate dielectric is stressed at a high field when the transistors are operating, so that it is demanded for gate dielectric to have excellent resistance to the impairment under long time stress at operating electric field. During high electric field stress, the carriers of leakage current and high electric field would impact the weak bonding, leading to more defects, higher leakage current and the degradation of transistor [32]. Therefore, the reliability of dielectric under gate bias stress would judge whether agrees with the application of gate dielectric. Figure 2-15 shows the variation of leakage current of different-treated SiO_x films as a function of stress time at a high electric field = 3.8 MV/cm, where I_0 is the initial leakage density. As well as the tendency of the measurement of breakdown voltage, the pure $SCCO_2$ fluids -treated SiOx film behaves the most rises in the degree of leakage current as the stress time increasing, because of the great amount of defects and weak bonding. However, after treating with 3000 psi-$SCCO_2$ process, the e-gun-deposited SiO_x film performs a fine reliability under high electric field stress, hence it is extremely suitable for the application of gate dielectric.

2.4 Summary

we have well improved the dielectric characteristics of e-gun deposited SiO_x films at 150 °C. From experimental results, the H_2O molecule is operative to react with Si dangling bonds, and the amount of S-O bonding in e-gun deposited SiO_x film increased obviously after H_2O vapor treatment. The preliminary improvement on electrical properties of SiO_x film was achieved due to the passivation of traps. A further study also demonstrated that $SCCO_2$ process mixed with co-solvent is optimum method to improve the dielectric characteristics of SiO_x film. In virtue of the gas-like and liquid-like properties, it is allowed for $SCCO_2$ fluid to transport H_2O molecules efficiently into SiO_x film and more of traps thereby were terminated. Additionally, the hysteresis-free in C-V curve was obtained, and it perhaps was a result of the removal of ion charges by the proposed $SCCO_2$ process.

Chapter 3

Application of Supercritical Fluid Technology on Resistive Random Access Memory

3.1 Fabrication of Non-volatile Memories and Experiment Process

Since the first observation of bistable resistance states in the 1960's, reversible and reproducible resistance switching phenomena caused by applied electric field have been investigated widely to be used as resistive random access memories (RRAM). Recently, numerous metal oxides and perovskite oxides including Nb_2O_5, TiO_2, and Nb-doped $SrTiO_3$ have been reported for RRAM applications. Nevertheless, there is only few studies mention the process of resistance memory at low temperature. the $SCCO_2$ fluid is proposed to fabricate the resistance memory at 150 °C, so it would be applicable to product RRAM on the substrates with low glass transition temperatures (T_g). The supercritical fluid technology is generally used for the impurity extraction, dehydration and drying of materials with a fine structure. It also had employed $SCCO_2$ fluid to deliver oxidant into metal oxide film for terminating electric defects by the gas-like and liquid-like properties. According to the mechanisms of bistable resistance states are possibly dominated by some kind of charge trap, the we would employ $SCCO_2$ technology to fabricate a resistance memory by varying the trap density in SiO_x film. The experimental works will focus on the effect of passivating traps by $SCCO_2$ treatment and investigate the influence of varying trap density on resistance switching phenomena.

Using the e-gun evaporation deposition method, the average thickness of 5-7 nm SiO_x films using pure SiO_2 target were directly deposited on p-type (100) silicon substrates having a resistivity of 1–10 Ωcm. During the deposition process, the chamber pressure and the substrate temperature were maintained at 2×10^{-6} torr and 25 °C, respectively. These SiO_x films were split into three groups and treated with different methods. The first group was placed in supercritical fluid system at 150 °C for 2 hrs, where was full of 3000 psi-$SCCO_2$ fluid, and taken as the control sample.Because the un-treated SiOx simple and pure 3000 psi-SCCO2 fluid were the same in current density-electric field characteristics.The second group was immersed into a pure H_2O vapor ambience at 150 °C for 2 hrs, in a pressure-proof stainless steel chamber. The third method was treated by 3000 psi-SCCO2 fluid mixed with 8 vol.% ethyl alcohol and 2 vol.% H_2O, where the H_2O is applied as oxidant to passivate electric defects in SiO_x film.The ethyl alcohol acted as a role of surfactant between nonpolar $SCCO_2$ fluid and polar H_2O molecule for making the uniform distribution of H_2O molecule in $SCCO_2$ fluids, so that the H_2O molecules could be effectively delivered into SiO_x layer by $SCCO_2$ fluids. After different treatments, the circle-shaped electrode of Al were thermally evaporated onto the surface of treated SiO_x films through a shadow mask to from the metal insulator semiconductor (MIS) structure, and the bottom electrode of Al were deposited onto the backside of p-type silicon substrates. The current-voltage (I-V) characteristics of MIS structure were measured by HP 4156-A semiconductor analyzer.

3.2 Analysis of Characteristics and Discussion

3.2.1 The current density-electric field (*J-E*) characteristics

Figure 3-1 shows the current density (*J*) of SiO_x film treated by 3000 psi $SCCO_2$ fluid as a function of bias voltage, the bias was applied on top electrode with grounded bottom electrode. In negative bias region, the plot of ln (J/E^2) versus reciprocal of electric field ($1/E$) is displayed in top right inset of Fig. 3-2. A linear dependence indicates the trap-assisted tunneling dominates current transport mechanism while applying larger negative bias than –0.8 V, as the schematic band diagram in bottom left inset of Fig. 3-1. Due to a large number of traps is present in the e-gun deposited SiO_x film, the high leakage current reaching about 10^{-1} A/cm^2 is observed at the bias of –2.5 V. In positive bias region, the electrons are generated mainly from (1) the interface states, (2) traps in depletion region, (3) bottom electrode of substrate. In this work, the generation of electrons from the bottom electrode of substrate or the traps in depletion region is negligible because of using p-type single-crystal Si as substrate. The saturate-like leakage current is caused from the interface states between SiO_x and Si substrate (as illustrated in bottom right inset of Fig. 3-1) and limited by the amount of interface states or the carrier generation rate, so the leakage current is lower than that under positive bias voltage. From these electrical behaviors, it is revealed that the pure CO_2 molecule is almost ineffective to passivate the traps originated from deposition process.

The current characteristic curves of SiO_x film treated by H_2O vapor is shown in Fig. 3-3, and it exhibits initially a high resistance state. Compared to the SiO_x film treated by pure $SCCO_2$ fluid, the leakage current is reduced obviously after H_2O vapor treatment. For further realize the reduction of leakage current, the leakage current density of high resistance state in negative bias region is analyzed according to Poole-Frenkel (P-F) emission, as shown in Fig. 3-4. The P-F emission is owing to field enhanced thermal excitation of trapped electrons in insulator onto the conduction band, and a schematic band diagram of P-F emission is drew in inset of Fig. 3-4. The linear trend in Fig. 3-4 expresses that the P-F emission dominates the conduction mechanism while applying larger negative bias than –1 V. The conversion of conduction mechanism from trap-assisted tunneling to P-F emission indicates parts of traps in e-gun deposited SiO_x layer were passivated by H_2O molecule during H_2O vapor process. Therefore, the lower leakage current is obtained in either negative bias or positive bias region. More interestingly, the H_2O vapor treated SiO_x film was found to exhibit a resistance switching of high resistance state (R_H) and low resistance state (R_L), and that was controllable by applied bias voltage. The voltages that switches the resistance state are about 1.8 V (from R_H to R_L) and –1.6 (from R_L to R_H), respectively. The maximum resistance ratio of two resistance states (R_H/R_L) is over 10^2 times at reading voltage (V_{read}) of 1 V. This phenomenon never occurs for the SiO_x film treated by pure $SCCO_2$ fluid.

Figure 3-5 displays the current characteristic curves of SiO_x film treated by 3000 psi $SCCO_2$ fluid mixed with ethyl alcohol and H_2O. Fig. 3-6 shows the plot of ln (J/E) versus square root of applied electric field ($E^{1/2}$) for the high resistance state in negative bias region. The current transport mechanism is dominated by Schottky-Richardson emission under low electric field and then dominated by P-F emission while applying larger negative bias than –2.4 V, as the schematic band diagram in inset of Fig. 3-6. The Schottky-Richardson emission, which is independent of traps, is caused by electron exciting thermally across the potential energy barrier via field assisted lowering at a metal–insulator interface. Under this treatment, the $SCCO_2$ fluid is a superior transporter to deliver H_2O molecule effectively into SiO_x layer, so that more of traps were passivated by H_2O molecule and the leakage current was suppressed further. Although the occurrence of P-F emission under high electric field indicates a few of traps remain in SiO_x film, the proposed $SCCO_2$ treatment is sufficient still to improve the quality of e-gun deposited SiO_x film. In addition, after this treatment, the SiO_x film performs a resistance switching behavior with higher bias voltage of switching resistance state.

3.2.2 Retention

Retention describes the ability to the NVM to store and recover information after a number of program cycles at a specified temperature. In any nonvolatile memory technology, it is essential to retain data for over ten years. This means the loss of charge stored in the storage medium must be as minimal as possible. For example, in modern Flash cells, FG capacitance is approximately 1 fF. A loss of only 1 fC can cause a 1V threshold voltage shift. If we consider the constraints on data retention in ten years, this means that a loss of less than five electrons per day can be tolerated [34]. Possible causes of charge loss are: (1) by tunneling or thermionic emission mechanisms; (2) defects in the tunnel oxide; and (3) detrapping of charge from insulating layers surrounding the storage medium; (4) mobile ion contamination. Further, the retention capability of Flash memories has to be checked by using accelerated tests that usually adopt screening electric fields and hostile environments at high temperature.But in this RRAM ,the current density was main electric characteristics The retention measurements are performed at room temperature by operating a 1 V gate voltage stress , The retention properties of different treated at H2O vapor and SCCO2-col demonstrated in Fig.3-7 and 3-8, respectively. This measurement is carried out using gate voltage stress.

3.2.3 Endurance

The term “endurance” refers to the ability of the nonvolatile memory to withstand repeated program cycles and still meet the specifications in the data sheet. In a conventional Flash memory the maximum number of erase/program cycles that the device must sustain is 10^5. Endurance characteristics for SCCO2 co-solvent treatment embedded in SiO_x film are shown in Fig. 3-9. Pulses (V_G - = ± 4 V,) were applied to evaluate endurance characteristics for the P/E operations.

3.2.4 Basic Program/Erase Mechanisms.

There were many references to express resistance transformation.The insulator silicon oxide to fabricate RRam mechanisms were introduced.(rederence paper) . the resistance of which is determined by the level and duration of the ion current above the electrodeposition threshold.During the reverse bias process ,the ion current flows in the opposite direction until the previously electrodeposited metal has been oxidized and returned to its original position o the oxidizable electrode. The resistance thereby increases until the device is returned to its original high resistance state. The sample with ahigh dielectric constant means that it owns high charge storagecapability. Because the electron transfer processes always accompanythe charge storage, the influence of dielectric constant becomes more important in MIM systems. Fig.3-10 illustrates howthe internal field affects the SET and RESET voltage for samples of various oxygen flow ratios. [35] If we pour the same voltage in two different permittivity samples, the real voltage in those samples will be different. For high permittivity sample, it can storage more charge in the interface and those charge form an opposite voltage in the insulator. Therefore, the real voltage in the sample was below the applied voltage. Similarly, there are few opposite voltage forms in the insulator of low permittivity sample. This might be explained due to the fact that the samples with few ratios needed more voltage to switch the state.

Figure 3-11 and 3-12 show the retention characteristics of two resistance states at room temperature for the SiO_x films treated by H_2O vapor and $SCCO_2$ fluid (mixed with ethyl alcohol and H_2O), respectively. The we think that the resistance change is possibly resulted from the movement of carrier between trap states in SiO_x gap, and a possible mechanism is shown in Fig. 3-12. As applying certain positive bias enough to make the tunneling of electrons in SiO_x gap, the energy band diagram would twist and lead to the resistance state transform from R_H to R_L. And the resistance state would return from R_L to R_H while applying certain negative bias enough to make these electrons tunneling back. If there are numerous traps exist in SiO_x gap, such as the pure $SCCO_2$ fluid treated SiO_x, these electrons could tunnel back without applying bias and result in no resistance state change. In other words, if there are only a few of traps exist in SiO_x gap, it would be required to apply higher bias voltage for shifting electrons, and excellent retention is also expected. Therefore, in contract to H_2O treated SiO_x film, the SiO_x film treated by $SCCO_2$ fluid mixed with ethyl alcohol and H_2O performs a higher bias voltage of switching resistance state and a longer retention time.

3.3 Summary

In summary, the preliminary improvement in properties of SiO_x films is obtained after H_2O vapor treatment because of passivating traps by H_2O molecule. A further study also demonstrated that the trap passivation efficiency is optimized by the treatment of $SCCO_2$ fluid mixed ethyl alcohol and H_2O, because the $SCCO_2$ fluid could effectively carry H_2O molecules into SiO_x film to terminate traps. On the other hand, it is found that the reduction of traps in SiO_x gap will induce a reversible resistance switching. The resistance change is possibly resulted from the carrier tunneling between internal states in SiO_x gap, so the number of traps would influence the bias voltage of switching resistance state and the retention time.

The further suppression of leakage current expresses that more of traps were terminated after the treatment of $SCCO_2$ fluid mixed with ethyl alcohol and H_2O. The higher bias voltage of switching the resistance state than that with H_2O vapor treatment is ascribed speculatively to the influence of trap density in SiO_x gap. The we think that the resistance change is possibly resulted from the movement of carrier between trap states in SiO_x gap.

Chapter 4

Conclusion

In this study, the dielectric characteristics of e-gun deposited SiO_x films at 150 °C. is improved from experimental results, the H_2O molecule is operative to react with Si dangling bonds, and the amount of S-O bonding in e-gun deposited SiO_x film increased obviously after H_2O vapor treatment. The preliminary improvement on electrical properties of SiO_x film was achieved due to the passivation of traps. A further study also demonstrated that $SCCO_2$ process mixed with co-solvent is optimum method to improve the dielectric characteristics of SiO_x film. In virtue of the gas-like and liquid-like properties, it is allowed for $SCCO_2$ fluid to transport H_2O molecules efficiently into SiO_x film and more of traps thereby were terminated. Additionally, the hysteresis-free in C-V curve was obtained, and it perhaps was a result of the removal of ion charges by the proposed $SCCO_2$ process.

On the other hand, it is found that the reduction of traps in SiO_x gap will induce a reversible resistance switching. The resistance change is possibly resulted from the carrier tunneling between internal states in SiO_x gap, so the number of traps would influence the bias voltage of switching resistance state and the retention time .The further suppression of leakage current expresses that more of traps were terminated after the treatment of $SCCO_2$ fluid mixed with ethyl alcohol and H_2O.The higher bias voltage of switching the resistance state than that with H_2O vapor treatment is ascribed speculatively to the influence of trap density in SiO_x gap. The we think that the resistance change is possibly resulted from the movement of carrier between trap states in SiO_x gap.

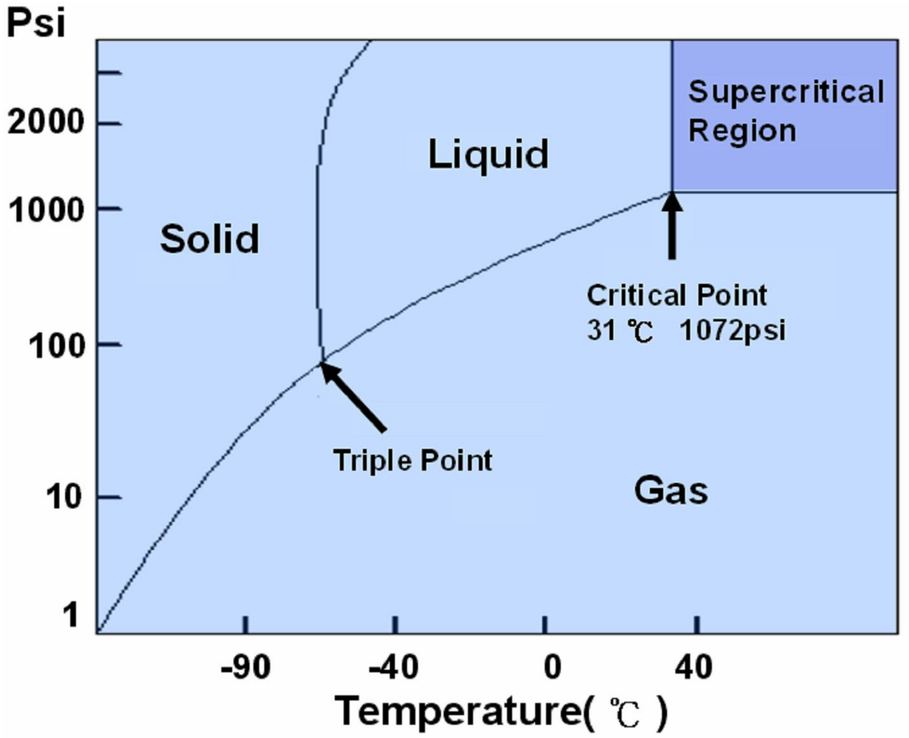

Fig. 1-1 Phase diagram for CO_2.

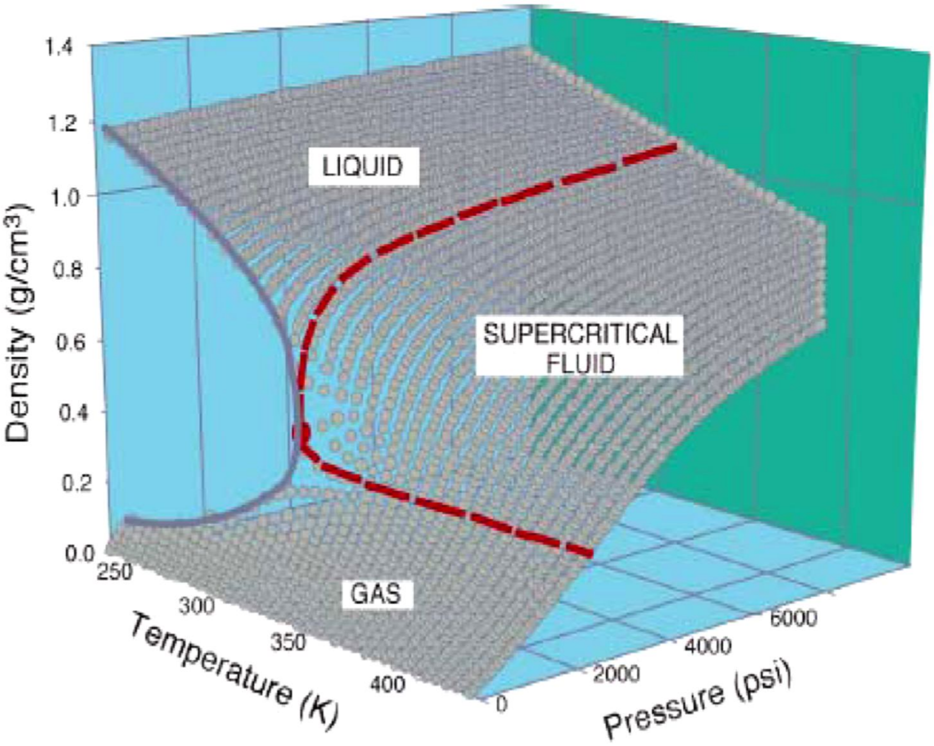

Fig. 1-2 Density-pressure-temperature surface for pure CO_2.

Fluid	Critical Temperature(℃)	Critical Pressure (Psi) (1atm=14.7psi)
Heliu (He)	-268	33
Neon (Ne)	-229	400
Argon (Ar)	-122	706
Nitrogen (N_2)	-147	492
Oxygen (O_2)	-119	731
Carbon dioxide (CO_2)	31	1072
Sulfur hexafluoride (SF_6)	46	545
Ammonia (NH_3)	133	1654
Water (H_2O)	374	3209

Table 1-1 Critical temperature and pressure for some common fluids.

	Liquid	**Supercritical Fluid**	**Vapor**
Density (g/cm^3)	**1.0**	**$0.3 \sim 0.7$**	**$\sim 10^{-3}$**
Diffusivity (cm^2/sec)	**$< 10^{-5}$**	**$10^{-2} \sim 10^{-5}$**	**$\sim 10^{-1}$**
Viscosity (g/cm-sec)	**$\sim 10^{-2}$**	**$10^{-3} \sim 10^{-6}$**	**$\sim 10^{-6}$**

Table 1-2 Comparison of physical properties of CO_2.

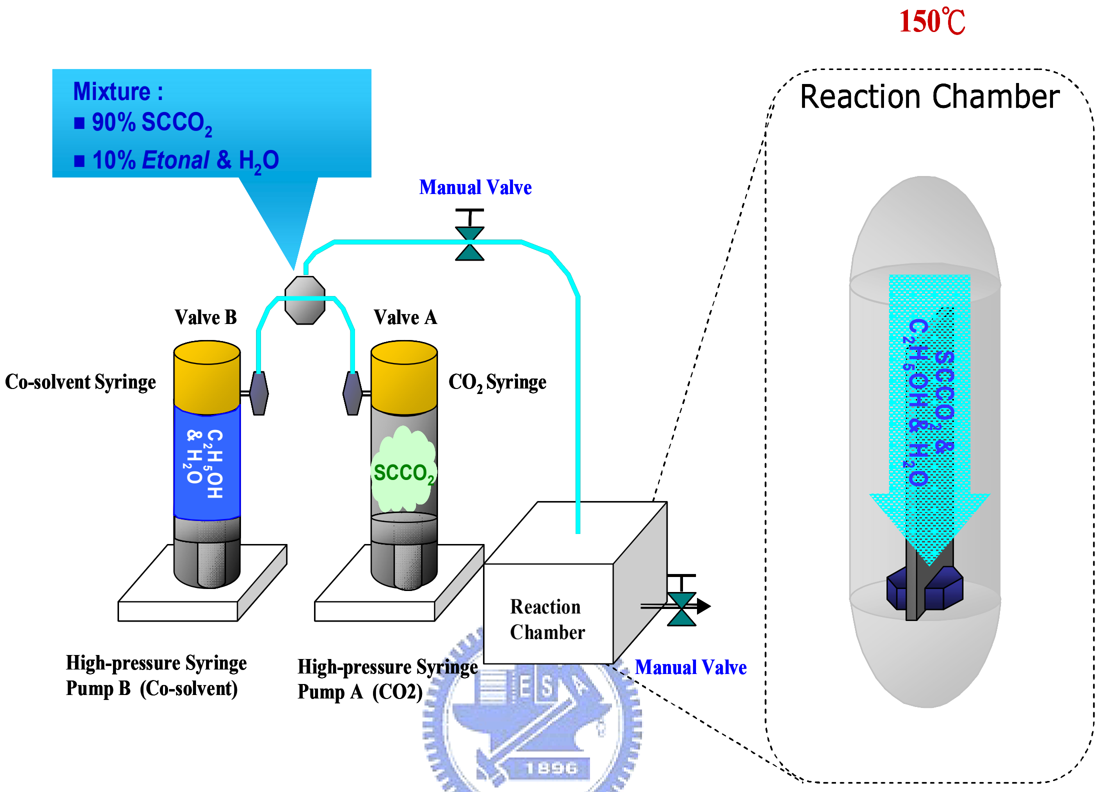

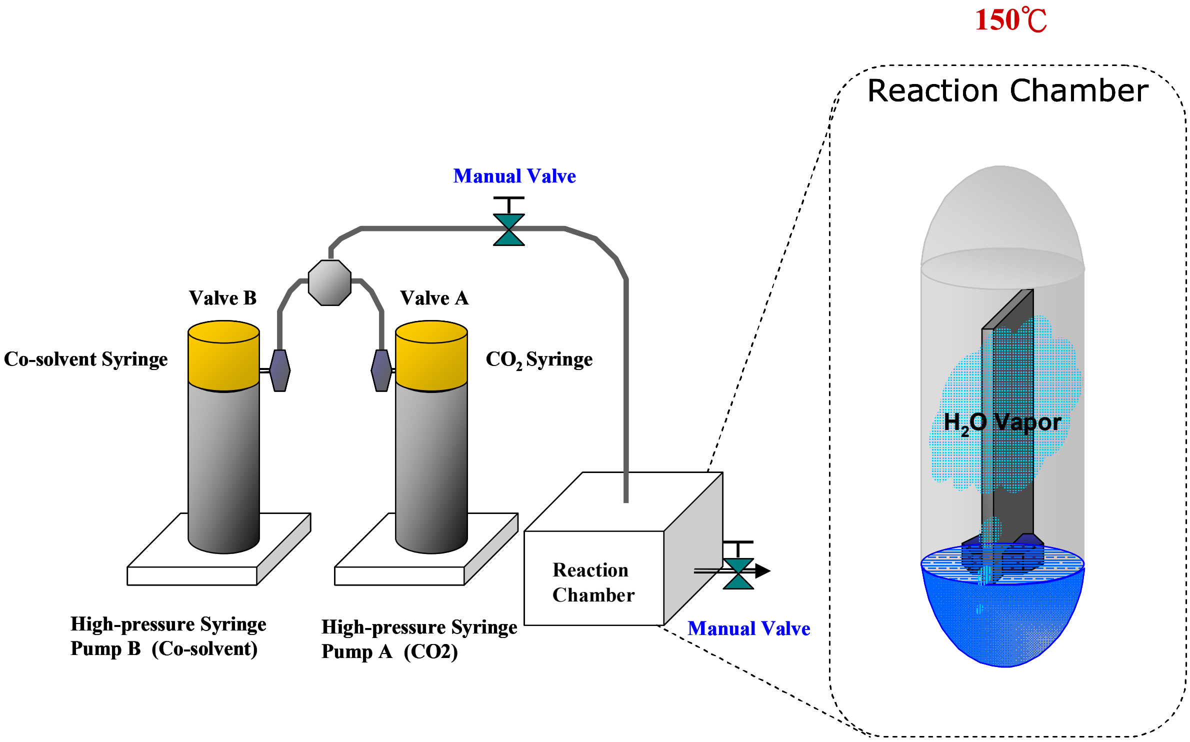

(b) H_2O-Vapor Treatment Process

Fig. 2-1 The supercritical fluid system.

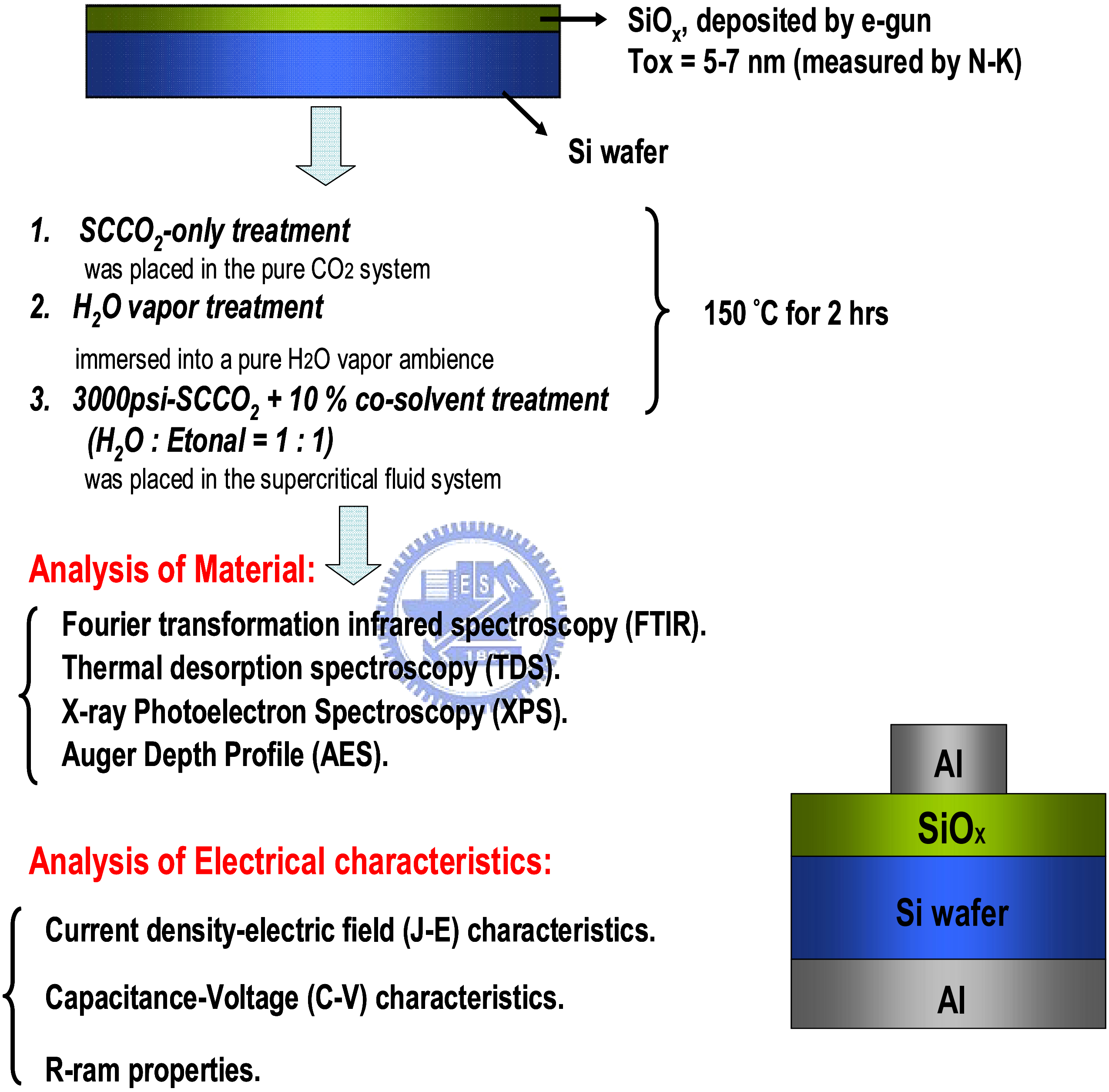

1. ***SCCO$_2$-only treatment***
   was placed in the pure CO2 system
2. ***H$_2$O vapor treatment***
   immersed into a pure H2O vapor ambience
3. ***3000psi-SCCO$_2$ + 10 % co-solvent treatment (H$_2$O : Etonal = 1 : 1)***
   was placed in the supercritical fluid system

Analysis of Material:

- **Fourier transformation infrared spectroscopy (FTIR).**
- **Thermal desorption spectroscopy (TDS).**
- **X-ray Photoelectron Spectroscopy (XPS).**
- **Auger Depth Profile (AES).**

Analysis of Electrical characteristics:

- **Current density-electric field (J-E) characteristics.**
- **Capacitance-Voltage (C-V) characteristics.**
- **R-ram properties.**

Fig. 2-2 The experiment processes of thin SiO$_x$ film with various treatments.

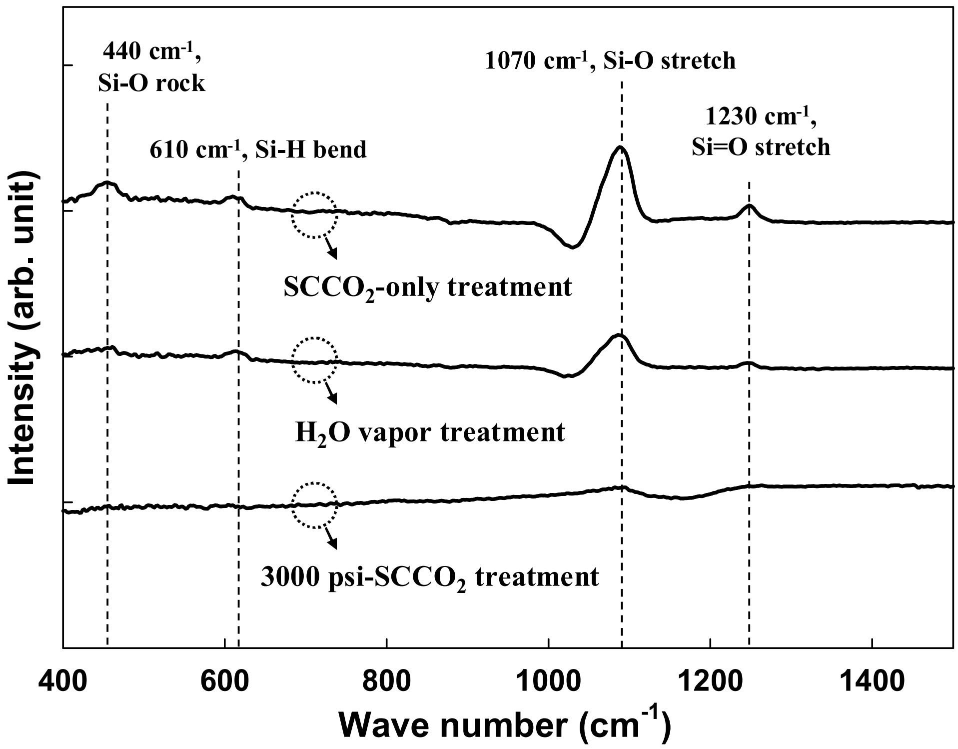

Fig. 2-3 The FTIR spectra of SiO_x films after various post-treatments, including $SCCO_2$-only, H_2O vapor and 3000psi-$SCCO_2$ treatment, and the un-treated SiO_x film is taken as background.

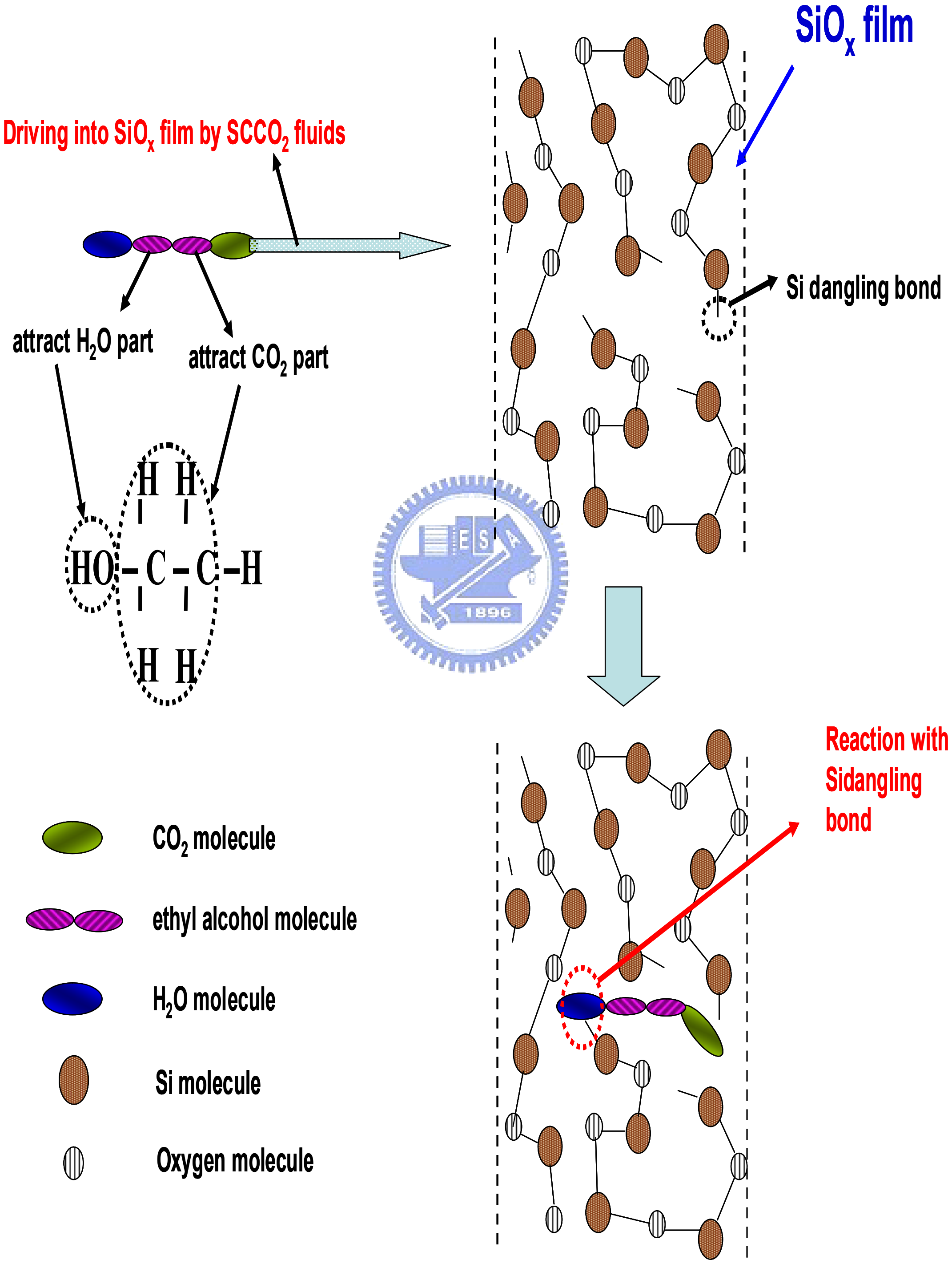

Fig. 2-4 The transporting mechanism for SCCO$_2$ fluids taking H_2O molecule into SiO$_x$ film.

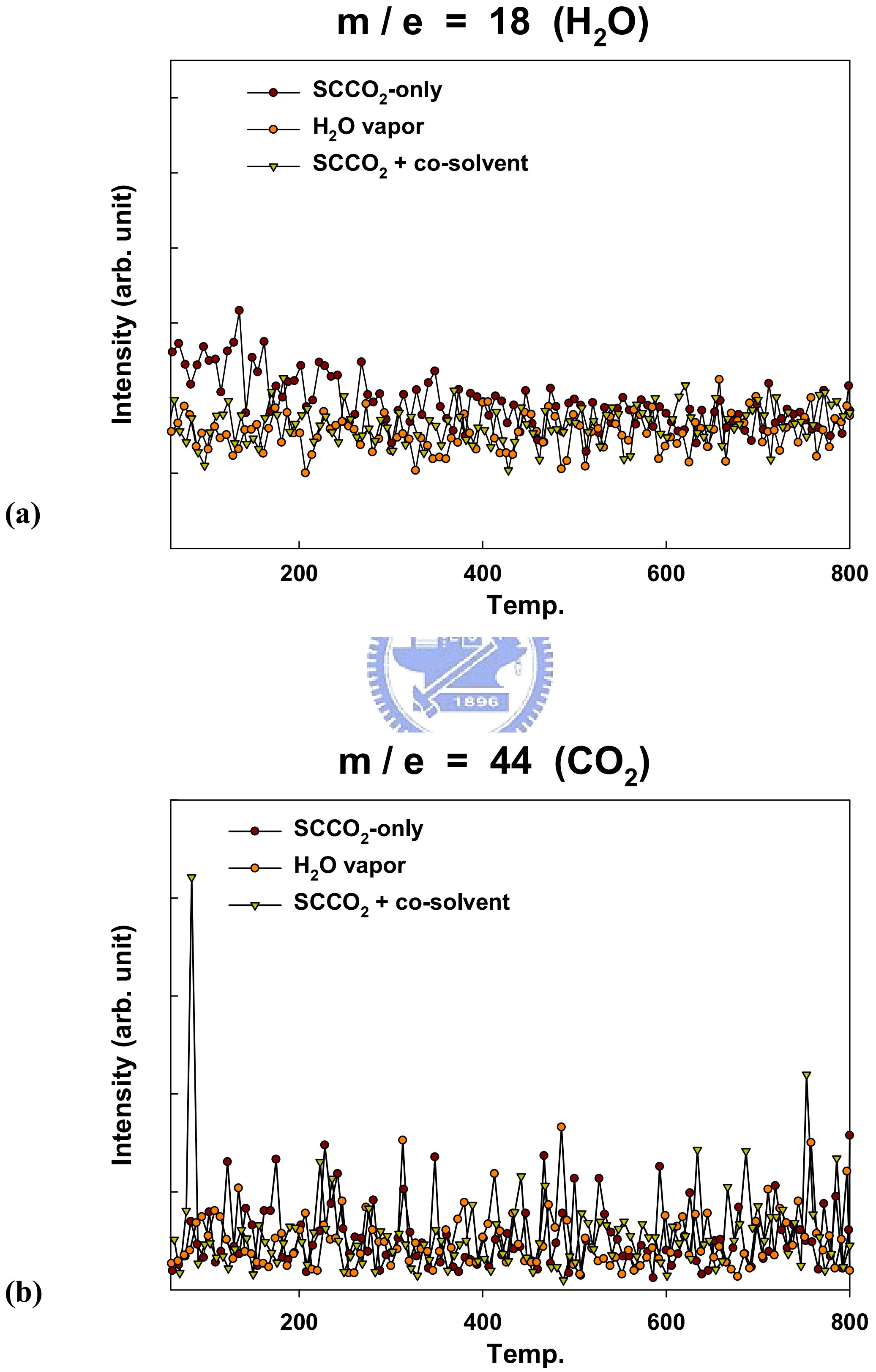

Fig. 2-5 The thermal desorption spectroscopy (TDS) measurement, (a) m/e (mass-to-charge ratio) = 18 peak that is attributed to H_2O, (b) m/e = 32 peak that is attributed to O_2.

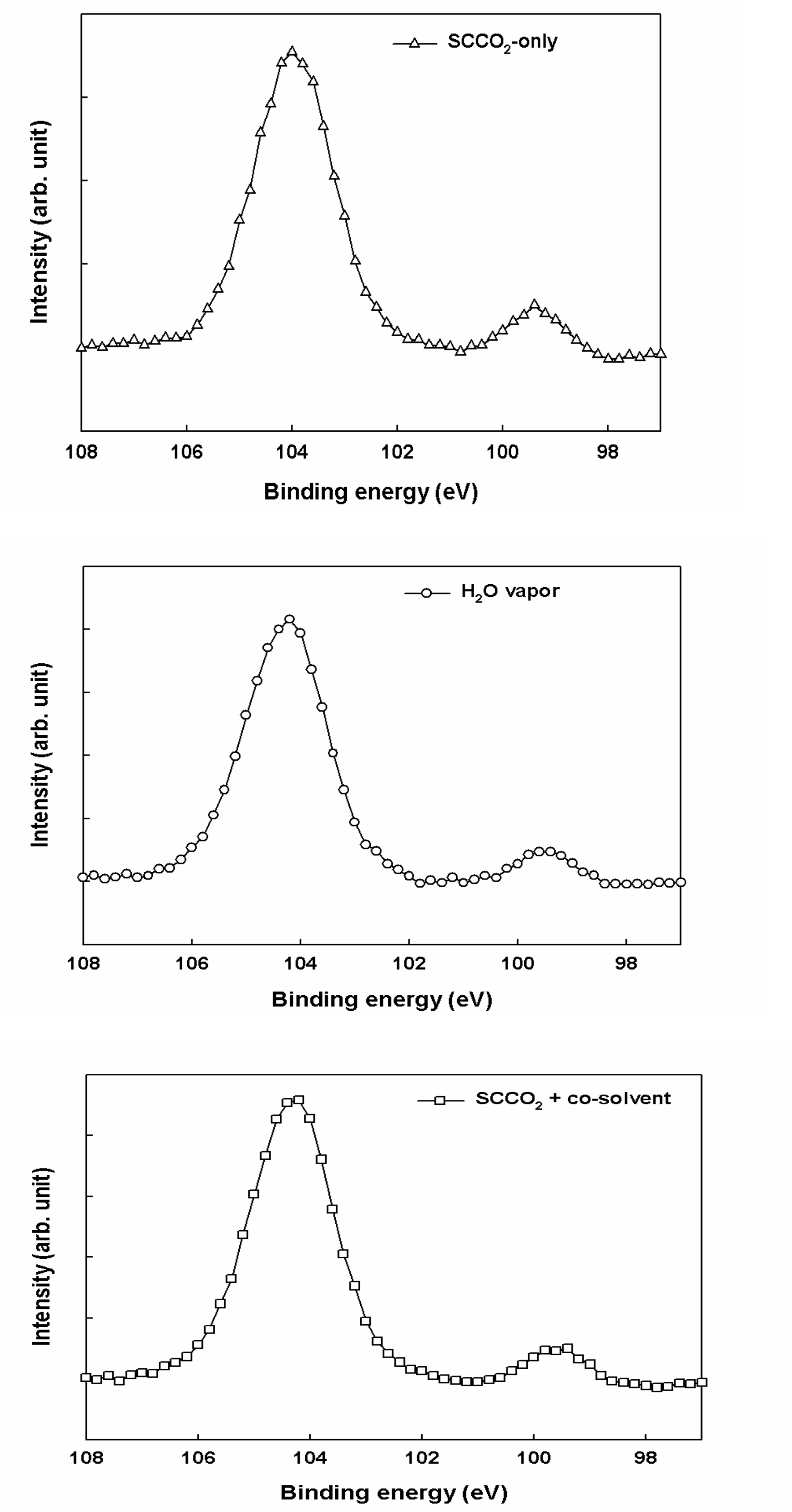

Fig. 2-6 The X-ray photoemission spectra of SiO_x films Si 2p after various post-treatments, including (a) $SCCO_2$-only, (b) H_2O vapor and (c) 3000psi-$SCCO_2$ treatment.

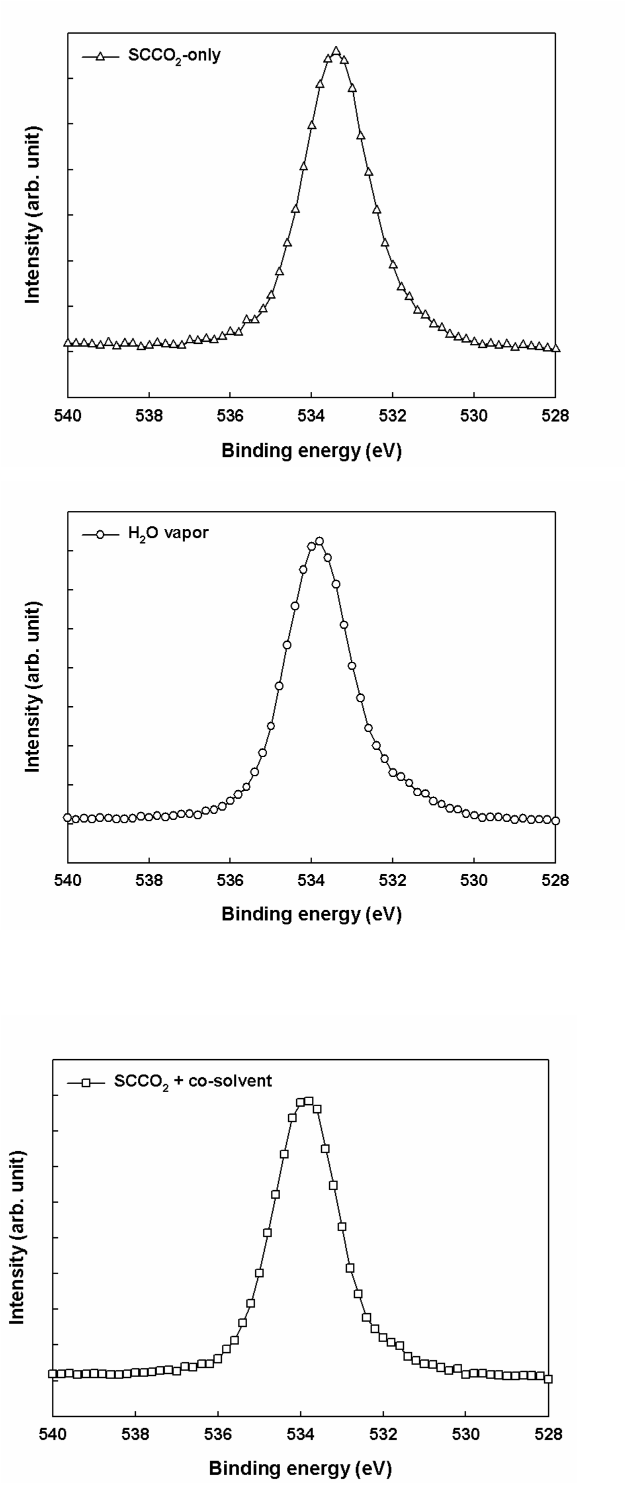

Fig. 2-7 The X-ray photoemission spectra of SiO_x films O 1s after various post-treatments, including (a) $SCCO_2$-only, (b) H_2O vapor and (c) 3000psi-$SCCO_2$ treatment.

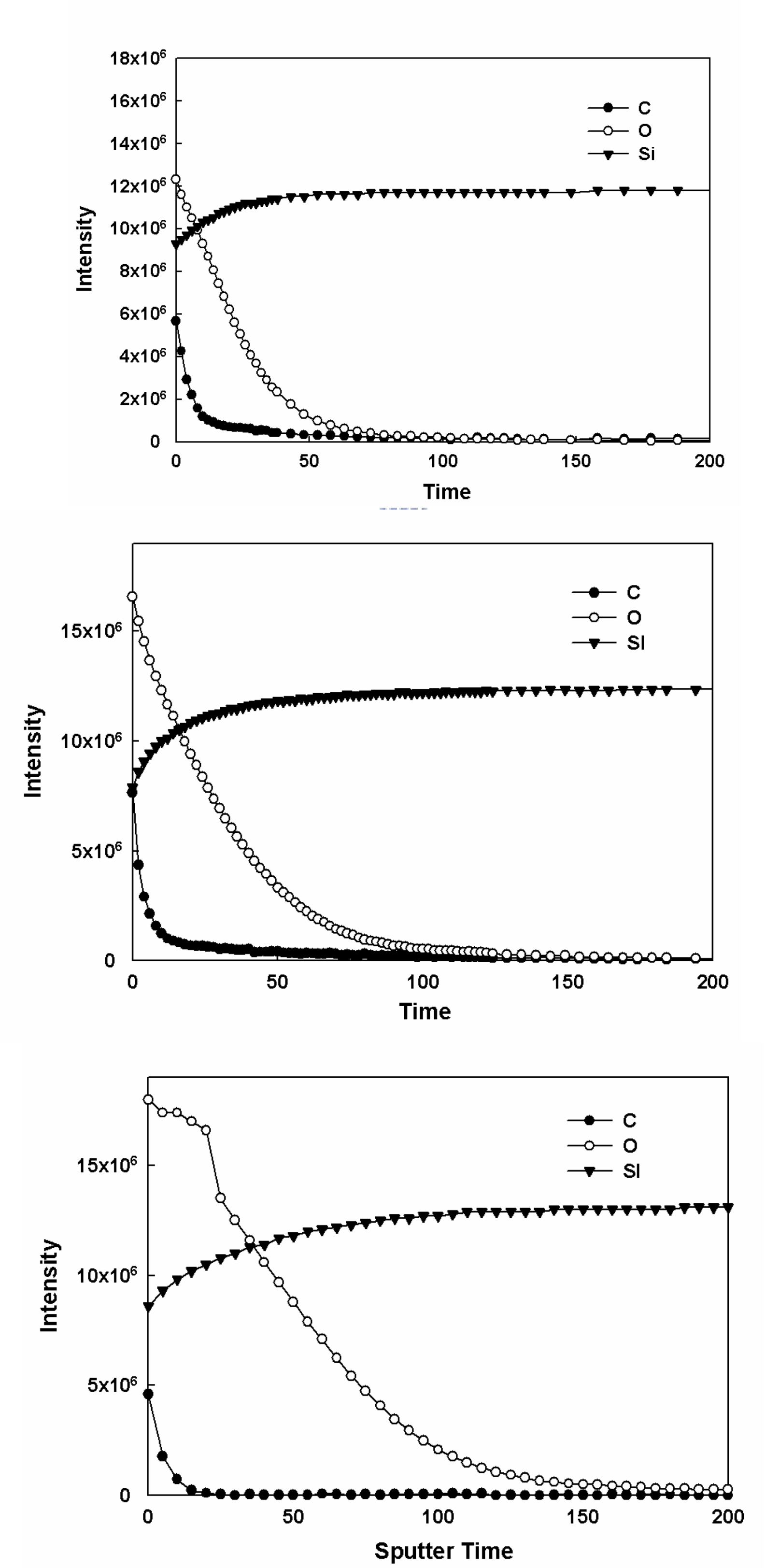

Fig. 2-8 Auger electron spectroscopy: (a) $SCCO_2$-only treatment (b) H_2O vapor treatment and (c) 3000psi-$SCCO_2$ treatment.

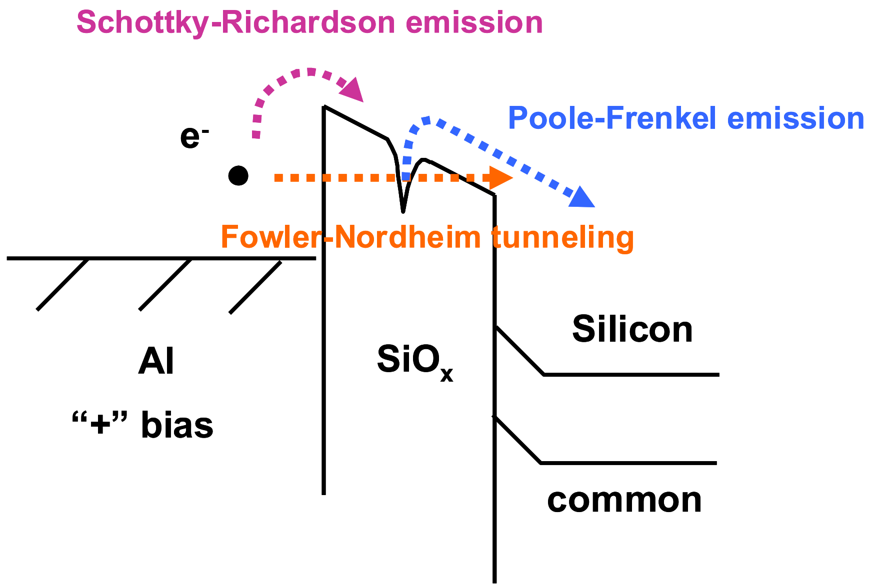

Fig. 2-9 Conduction mechanism for Al/SiO_x/Si MIS structure.

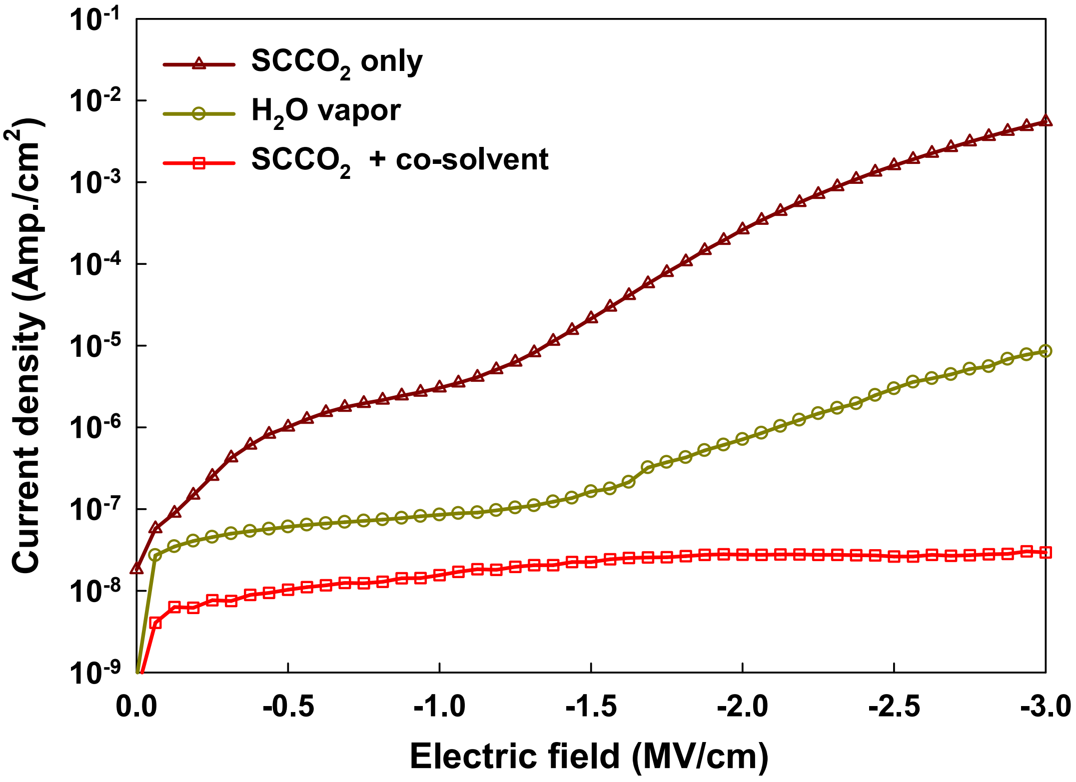

Fig. 2-10 The leakage current densities of SiO_x films after different treatments. (The negative bias is applied on gate electrode)

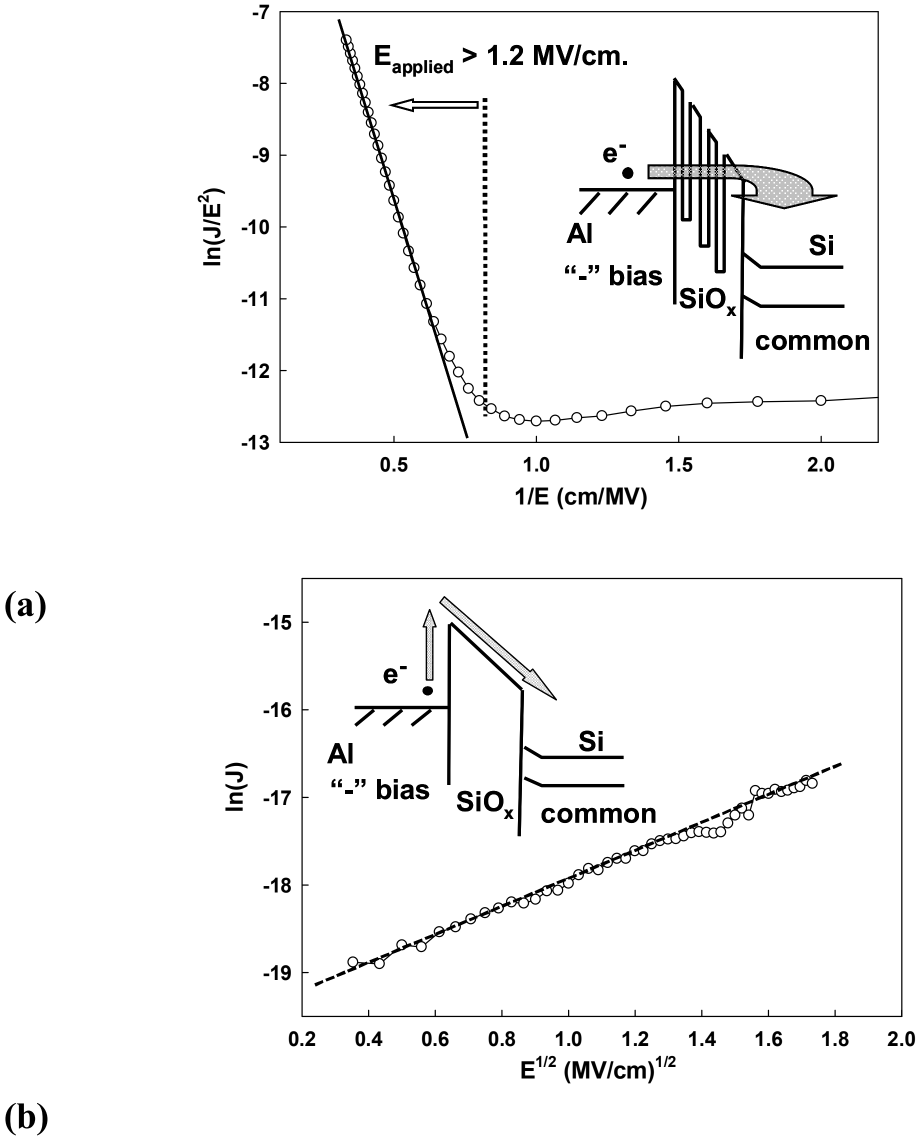

Fig. 2-11 (a) Curve of ln (J/E) versus reciprocal of electric field (*1/E*) for the $SCCO_2$-only treated SiO_x film, and a schematic energy band diagram accounting for trap-assisted tunneling shown in the inset. (b) Leakage current density versus the square root of electric field ($E^{1/2}$) plot for the 3000 psi-$SCCO_2$ treated SiO_x film. The inset shows the energy band diagram of Schottky-type conduction mechanism.

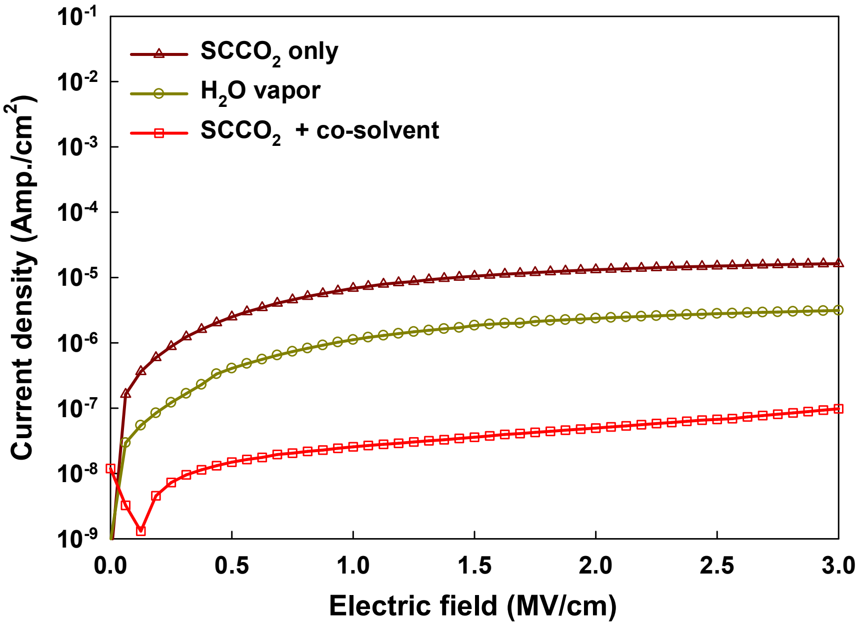

Fig. 2-12 The leakage current densities of SiO$_x$ films after different treatments (The positive bias is applied on gate electrode). Inset plots the energy band diagram of leakage current.

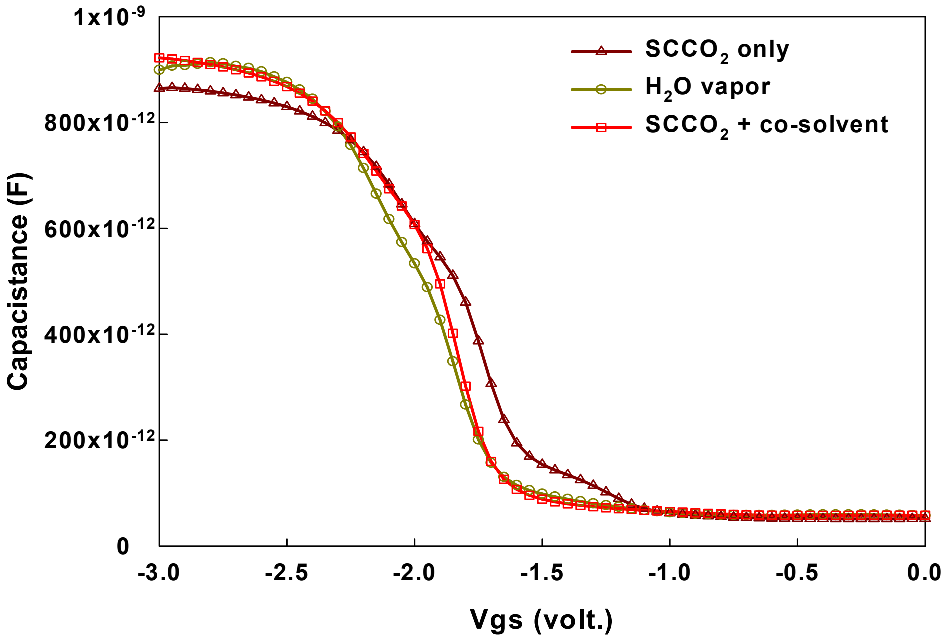

Fig. 2-13 The capacitance-voltage characteristics of SiO$_x$ films after different treatment, measuring at 1M Hz with gate bias swing

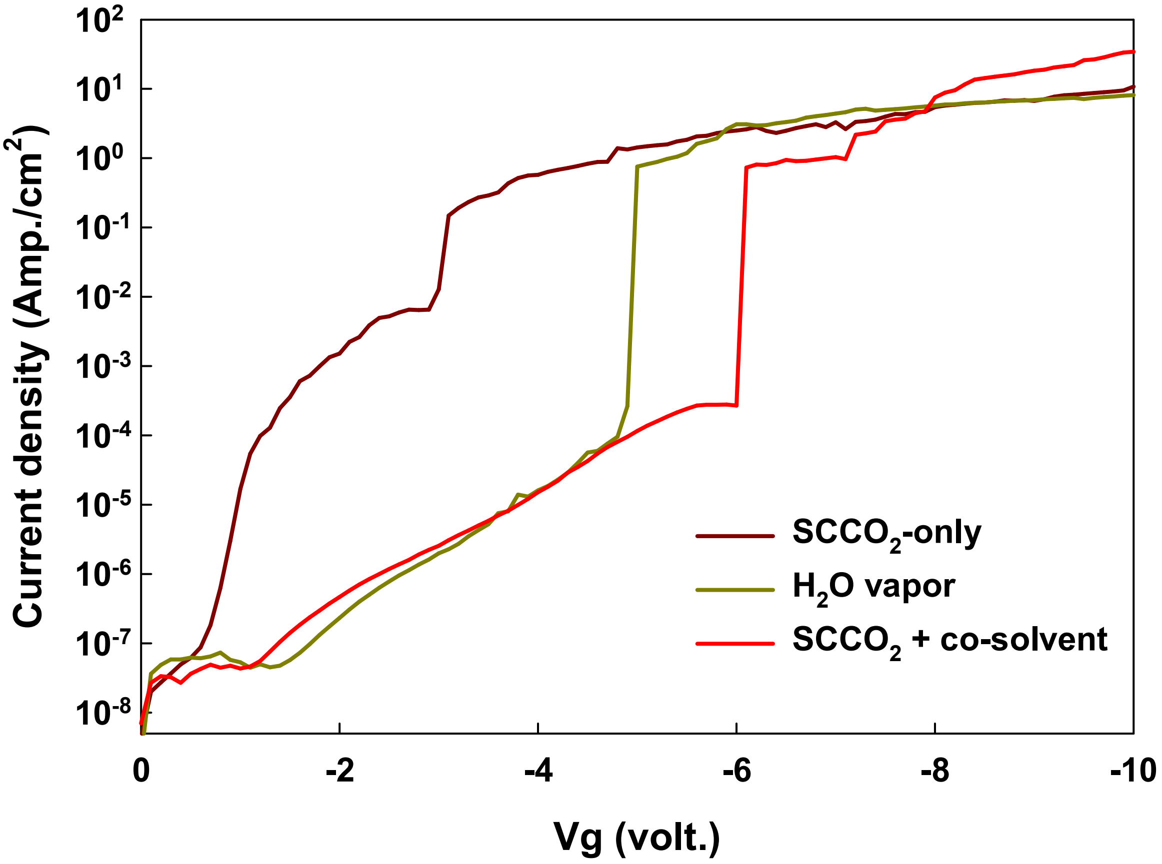

Fig. 2-14 The breakdown characteristic curves of SiO$_x$ films after various treatments at negative gate bias region.

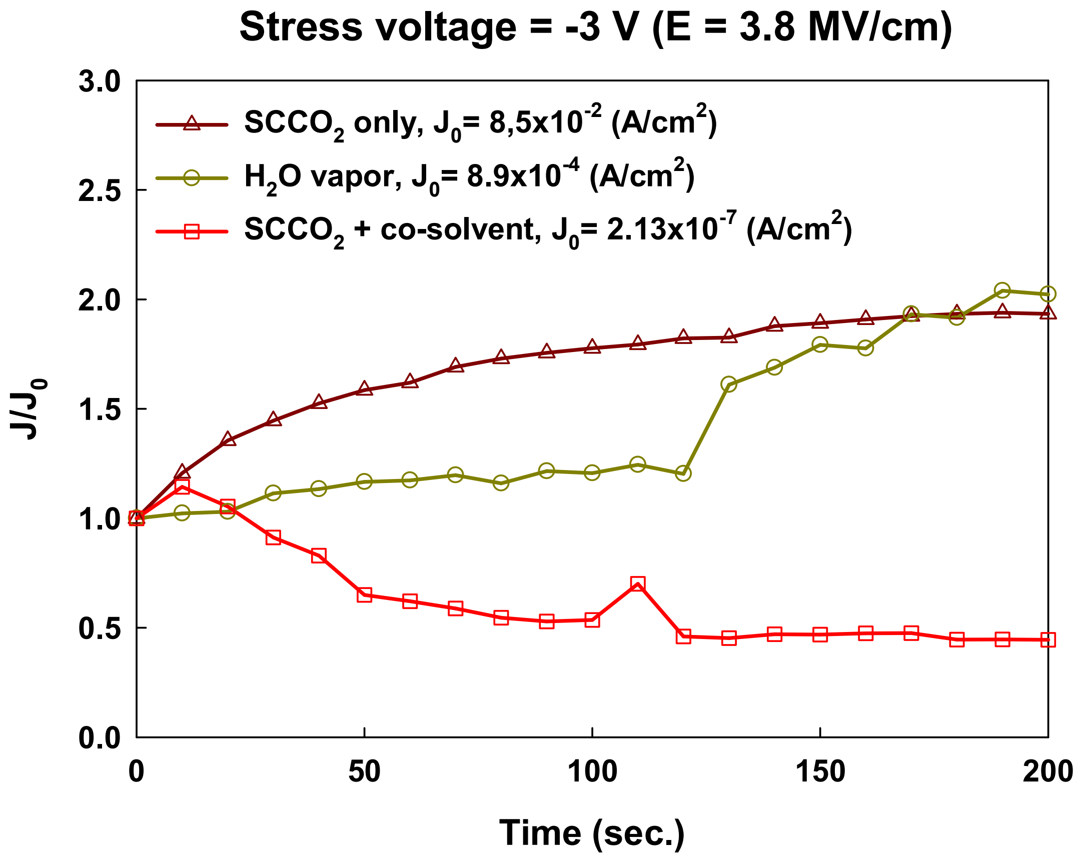

Fig. 2-15 The variation of leakage current of different-treated SiO_x films as a function of stress time at a high electric field = 3.8 MV/cm.

	Si-O	Si-Si
SCCO2-only	103.8	99.5
H_2O-vapor	104.0	99.5
3000psi-$SCCO_2$	104.1	99.5

Table 2-1 Summary of binding energies for ultra thin SiO_x films Si2p after various post-treatments, including SCCO2-only, H_2O vapor and 3000psi-$SCCO_2$ treatment.

	Si-O
$SCCO_2$-only	533
H_2O-vapor	534
3000psi-$SCCO_2$	534

Table 2-2 Summary of binding energies for ultra thin SiO_x films O 1s after various post-treatments, including $SCCO_2$-only, H_2O vapor and 3000psi-$SCCO_2$ treatment.

	Dielectric constant
$SCCO_2$ only	3.57
H_2O vapor	3.74
$SCCO_2$+ co-solvent	3.8

Table 2-3 The extracted parameters from C-V curves of SiO_x films after different treatment

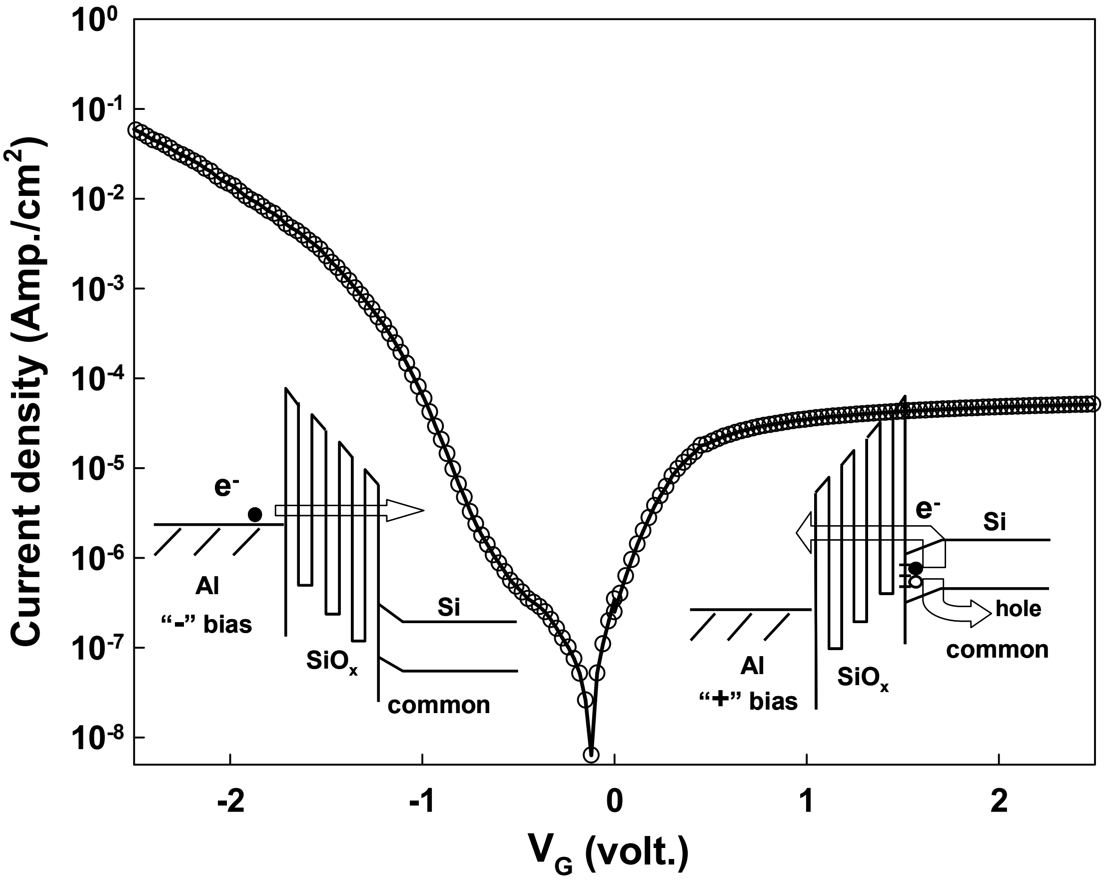

Fig. 3-1 shows the current density (*J*) of SiO_x film treated by 3000 psi $SCCO_2$ fluid as a function of bias voltage

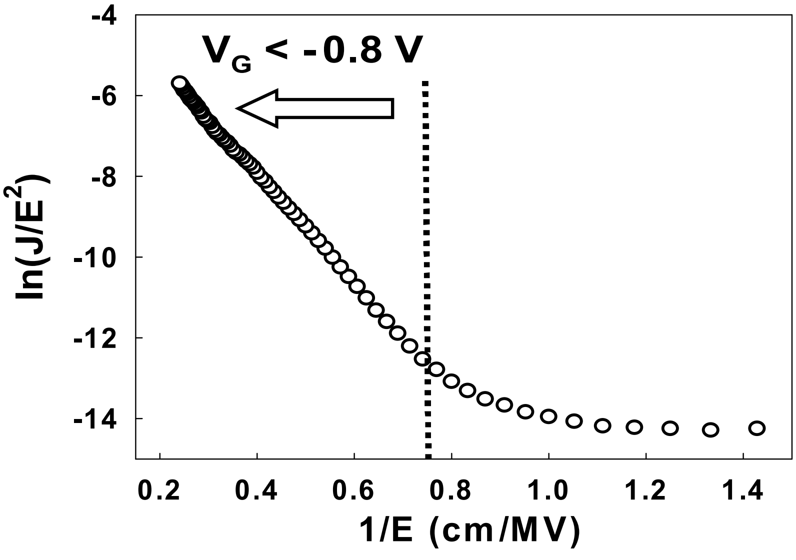

Fig. 3-2 A linear dependence indicates the trap-assisted tunneling dominates current transport mechanism while applying larger negative bias than –0.8 V

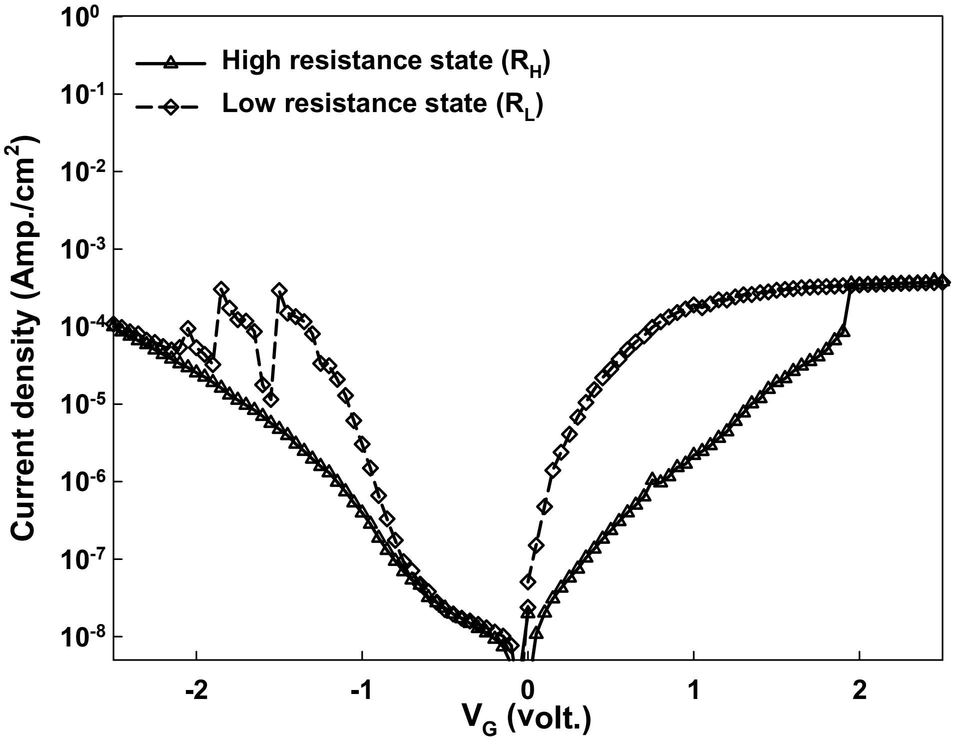

Fig. 3-3 The current characteristic curves of SiO_x film treated by H_2O vapor

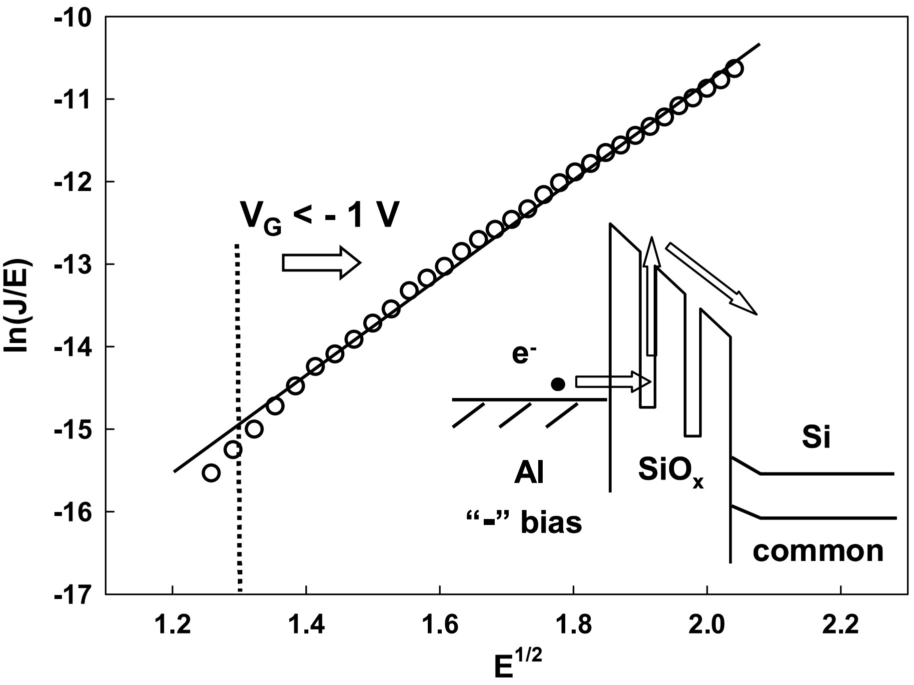

Fig. 3-4 the P-F emission dominates the conduction mechanism while applying larger negative bias than –1 V

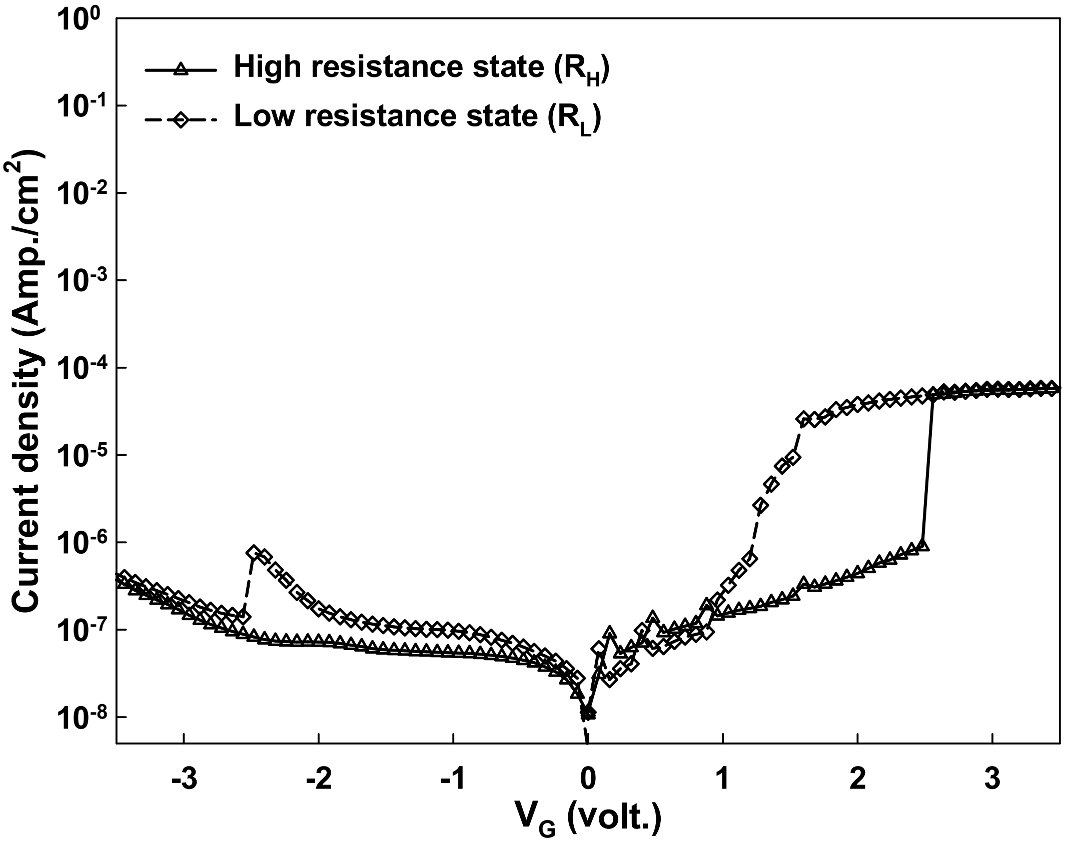

Fig. 3-5 displays the current characteristic curves of SiO_x film treated by 3000 psi $SCCO_2$ fluid mixed with ethyl alcohol and H_2O.

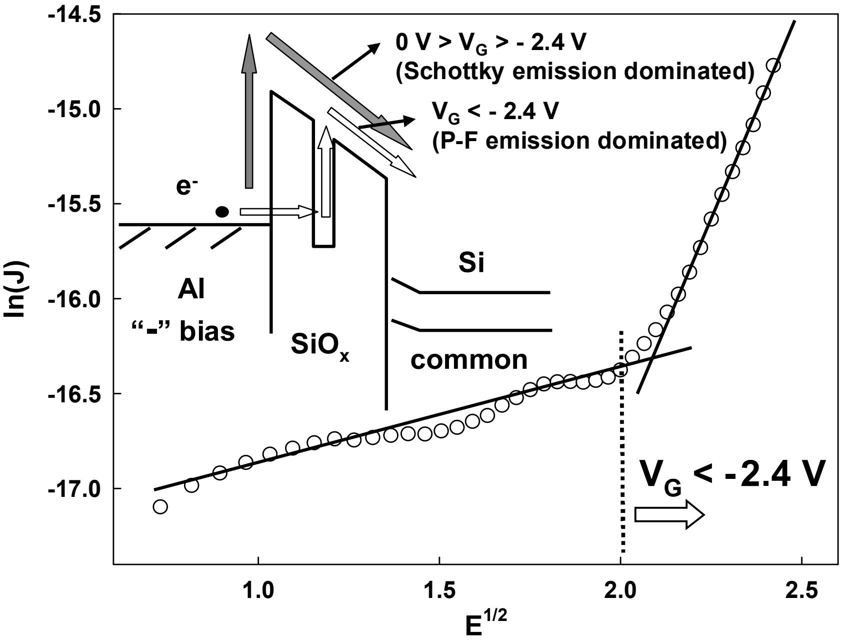

Fig. 3-6 the plot of ln (J/E) versus square root of applied electric field ($E^{1/2}$)

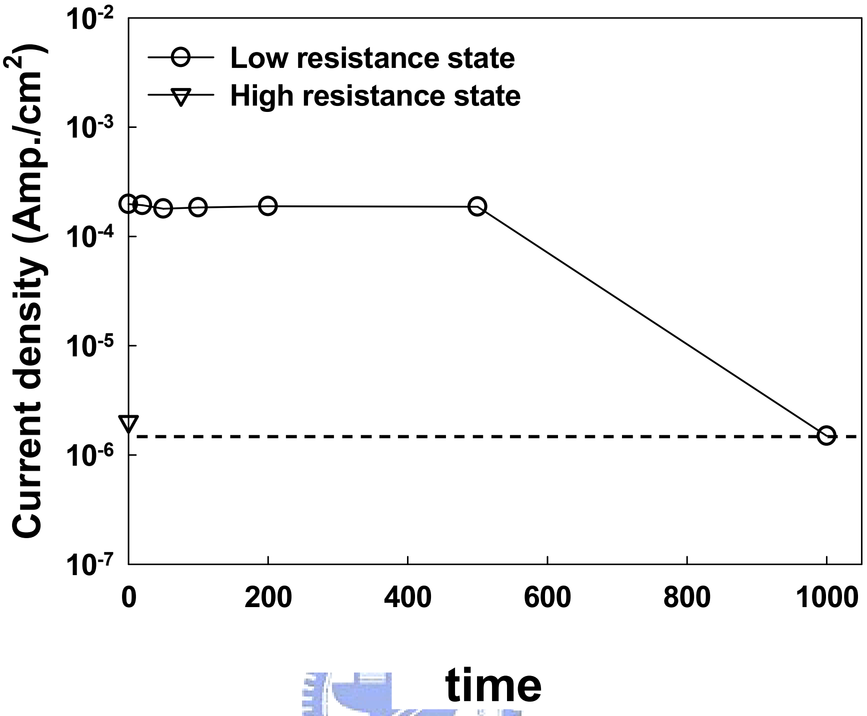

Fig. 3-7 The retention properties reated at H2O vapor

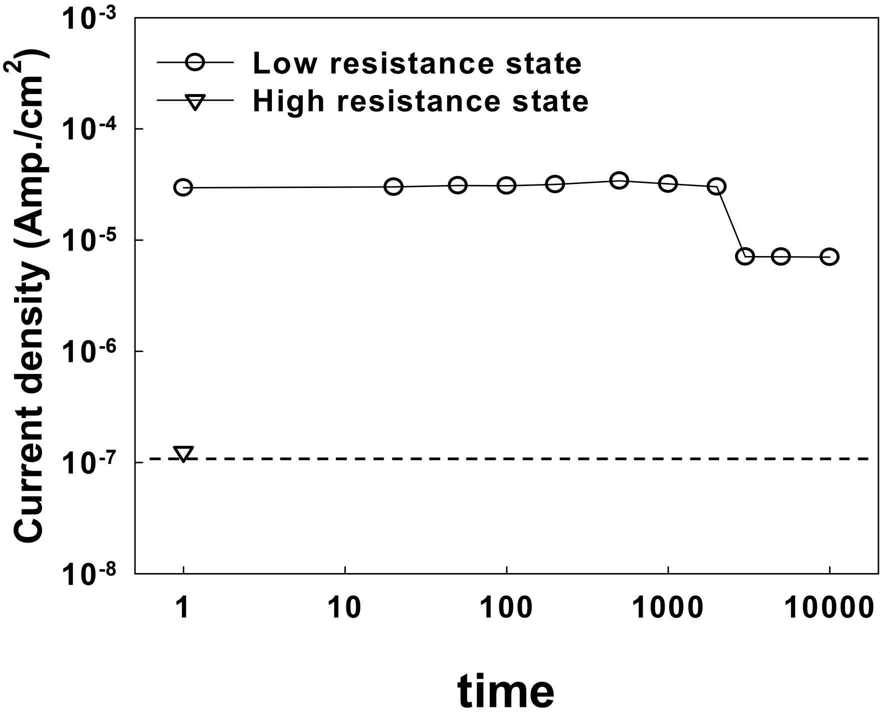

Fig. 3-8 The retention properties treated at SCCO2-col

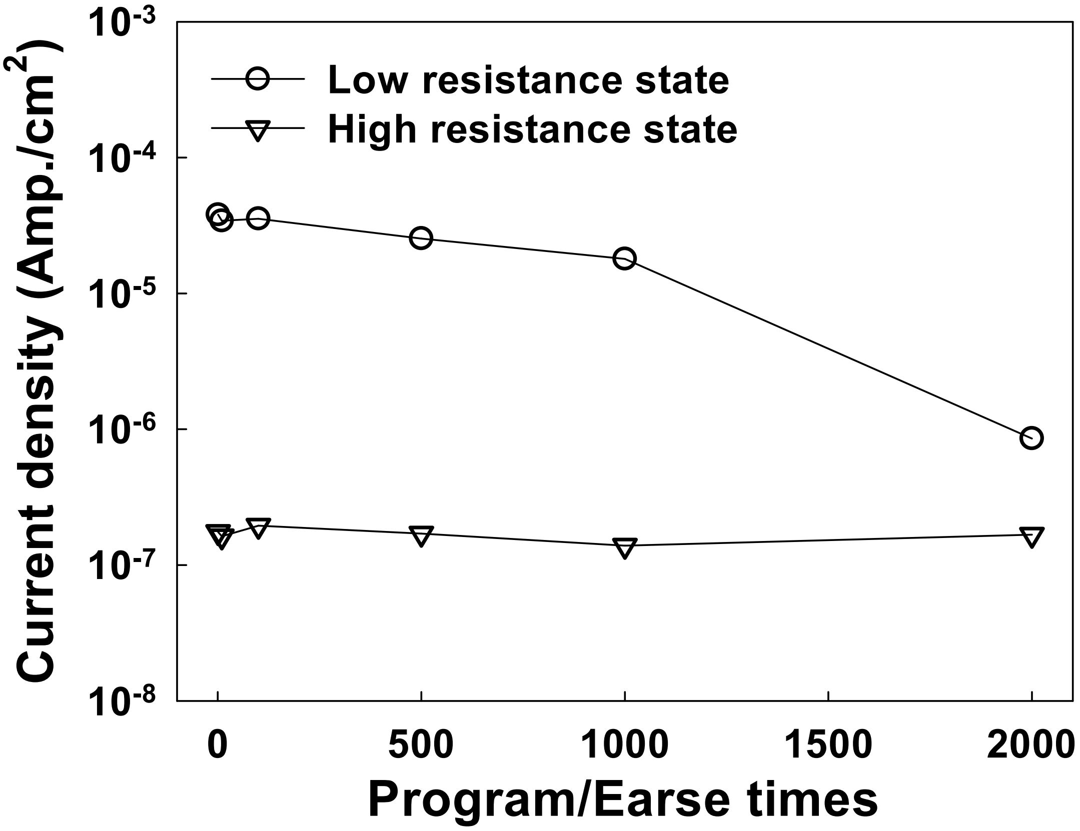

Fig. 3-9 Endurance for SCCO2 co-solvent treatment embedded in SiO_x film

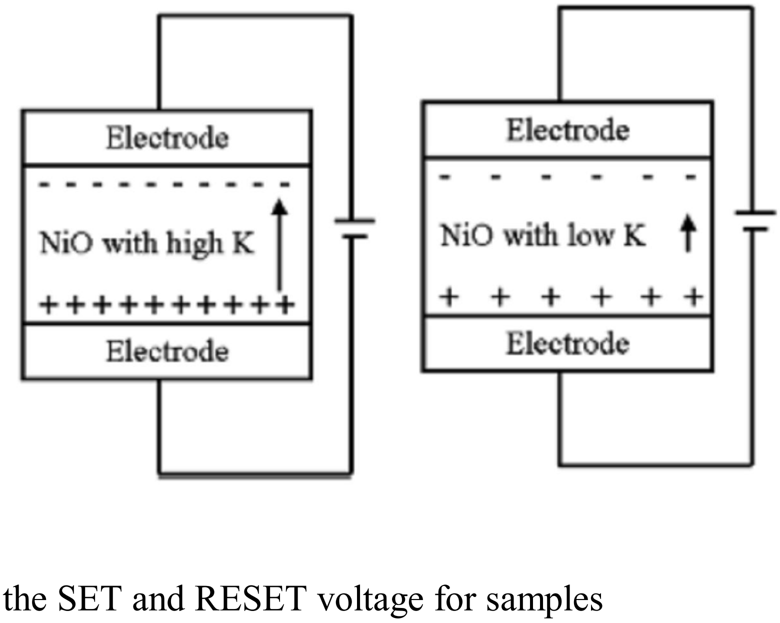

Fig. 3-10 the SET and RESET voltage for samples

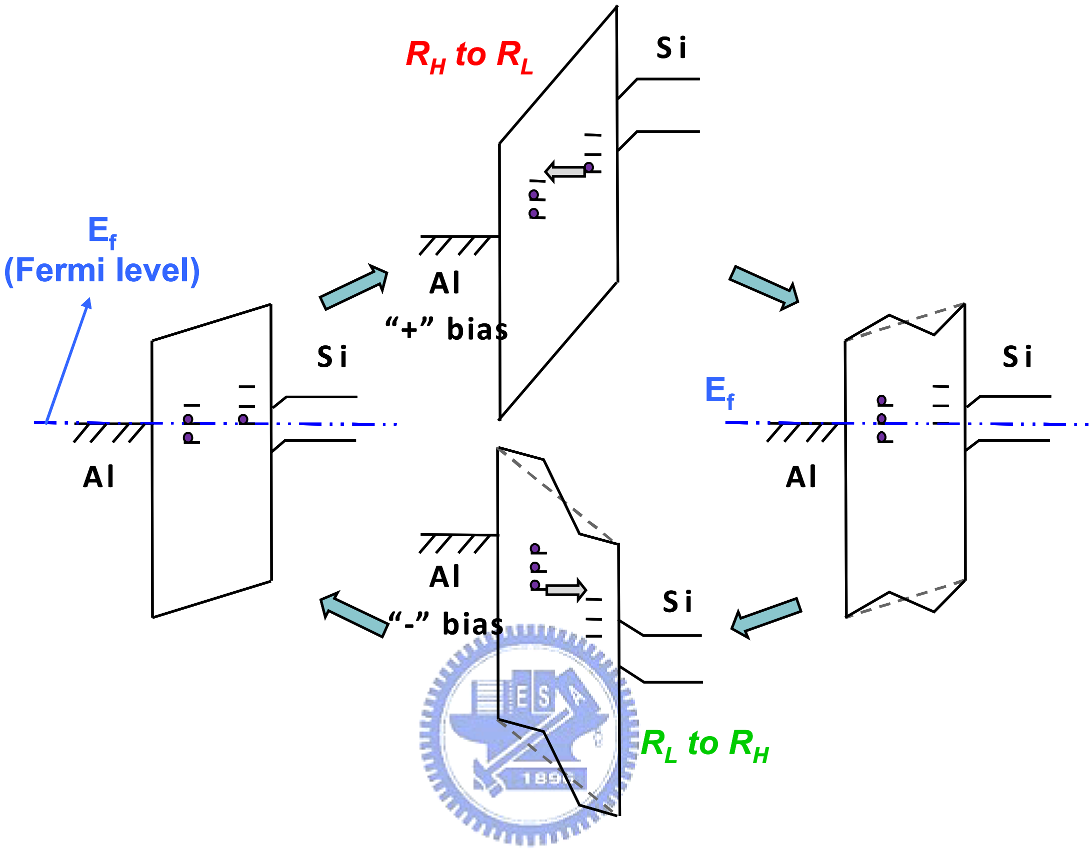

Fig. 3-11 show the retention characteristics of two resistance states at room temperature for the SiO_x films

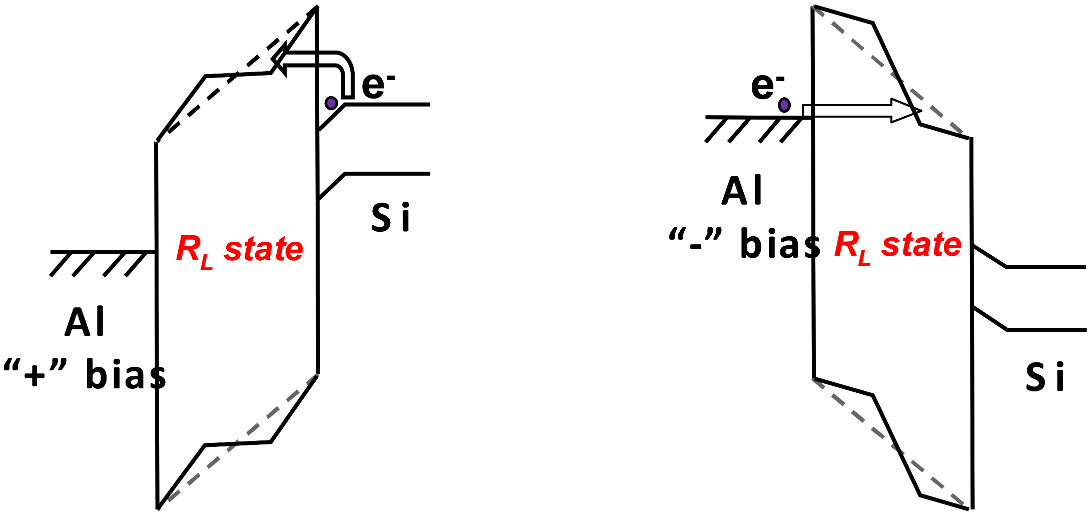

Fig. 3-12 movement of carrier between trap states in SiO_x gap, and a possible mechanism

References

[1] K. Zosel, and Angew. *Chem. Int. Ed. Engl*, vol. 17, pp. 702, 1978.

[2] P. M. F. Paul, and W. S. Wise, *Mills&Boon, Ltd*, 1971.

[3] J. F. Brennecke, and C. A. Eckert, *AIChEJ*, vol. 35, pp1049, 1989.

[4] J. B. Rubin, L. B. Davenhall, C. M. V. Taylor, L. D. Sivils, T. Pierce, and K. Tiefert, *International LANL*, 1998.

[5] L. B. Rothman, R. J. Robey, M. K. Ali, and D. J. Mount, *IEEE/SEMI Advanced Semiconductor manufacturing Conference*, 2002.

[6] W. H. Mullee, M. A. Biberger, and P. E. Schilling, *United States Patent*, Patent 6500605 B1, 2002.

[7] G. D. Wilk, R. M. Wallace, and J. M. Anthony, *J. Appl. Phys.*,**89(10)**, 5243 (2001).

[8] E. E. Crisman, J. I. Lee, P. J. Stiles, and O. J. Gregory, *IEEE Electronics Lett.*, **23(1)**, 8 (1987)..

[9] C. H. Lee, S. H. Hur, Y. C. Shin, J. H. Choi, D. G. Park, and K. Kim, *Appl. Phys. Lett.*, **86**, 152908 (2005).

[10] Ming-Daou Lee[1], Chia-Hua Ho[2], Chi-Kuen Lo[3], Tai-Yen Peng[1], Yeong-Der Yao[4] IEEE, VOL. 43, NO. 2, FEBRUARY 2007

[11] S. K. Park, Y. H. Kim, J. I. Han, D. G. Moon, and W. K. Kim, *IEEE Trans. Electron Devices*, **49(11)**, 2008 (2002).

[12] A. Sazonov and C. McArthur, *J. Vac. Sci. Technol. A*, **22(5)**, 2052 (2004).

[13] C. S. Yang, L. L. Smith, C. B. Arthur, and G. N. Parsons, *J. Vac. Sci. Technol. B*, **18(2)**, 683 (2000).

[14] M. Liu, Q. Fang, G. He, L. Q. Zhu, and L. D. Zhang, *J. Appl. Phys.*, vol. 101, 034107, 2007.

[15] H. Watakabe, T. Sameshima, T. Strutz, T. Oitome and A. Kohno, *Jap. J. Appl. Phys.*, **44(12)**, 8367 (2005).

[16] N. Sano, M. Sekiya, M. Hara, A. Kohno, and T. Sameshima, *Appl. Phys. Lett.*, **66(16)**, 2107 (1995).

[17] P.S. Bagus, F. Illas, G. Paccghioni, F. Parmigiani, J. Electron Spectrosc. Related Phenom. 100 (1999) 215.

[18] Hollinger G.. Appl. Surf. Sci. 8, 318 (1981)

[19] Cros A., Saoudi R., Hewett C.A., Lau S.S., Hollinger G. J. Appl. Phys. 67, 1826 (1990)

[20] Bell F.G., Ley L Phys. Rev. B 37, 8383 (1988)

[21] Montero I., Galan L., de la Cal E., Albella J.M., Pivin J.C. Thin Solid Films 193, 325 (1990)

[22] Edgell M.J., Baer D.R., Castle J.E. Appl. Surf. Sci. 26, 129 (1986)

[23] W. J. Zhu, Tso-Ping Ma, Takashi Tamagawa, J. Kim, and Y. Di, *IEEE Electron Devices Lett*. vol. 23, No. 2, 2002.

[24] Takeshi Yamaguchi, Hideki Satake, and Noburu Fukushima, *IEEE Trans. Electron Devices*, vol. 51, No. 5, 2004.

[25] M. Houssa, M. Tuominen, et al., *J. Appl. Phys.*, vol. 87, No. 12, pp. 8615, 2000.

[26] Sanghun Jeon, Hyundoek Yang, Dae-Gyu Park, and Hyunsang Hwang, *Jpn. J. Appl. Phys.*, vol. 31, pp. 2390-2393, 2002.

[27] Dieter K. Schrodr, Wiley-INTERSCIENCE, 1998.

[28] M. Lenzlinger, and E. H. Snow, *J. Appl. Phys.*, vol. 40, pp. 278, 1969.

[29] R. Mahapatra, A. K. Chakraborty, N. Poolamai, A. Horsfall, S. Chattopadhyay, and N. G. Wright, *J. Vac. Sci. Technol. B*, vol. 25(1), pp. 217, 2007.

[30] P. R. Emtage, and W. Tantraporn, *Phys. Rev. Lett.*, vol. 8, pp. 267, 1962.

[31] J. R. Yeargan, and H. L. Taylor, *J. Appl. Phys.*, vol. 39, pp. 5600, 1968.

[32] T. F F. Crupi, R. Degraeve, A. Kerber, D. H. Kwak, and G. Groeseneken, *IEEE 42nd Annual International Reliability Physics Symposium*, pp. 181, 2004

[33] S. W. Huang, and J. G. Hwu, *IEEE Trans. Electron Devices*, vol. 50, pp. 1658, 2003.

[34] P. Pavan, R. Bez, P. Olivo, and E. Zanoni, Proceedings of The IEEE, 85, 1248 (1997)

[35] Ming-Daou Lee1, Chia-Hua Ho2, Chi-Kuen Lo3, Tai-Yen Peng1, and Yeong-Der Yao4IEEE TRANSACTIONS ON MAGNETICS, VOL. 43, NO. 2, FEBRUARY 2007

[36] C. T. Tsai, T. C. Chang, P. T. Liu, P. Y. Yang, Y. C. Kuoand, K. T. Kin, P. L. Chang, and F. S. Huang, *Appl. Phys. Lett.*, **91**, 012109 (2007).

簡歷

姓名：鄭逸立 (Yi-Li Cheng)

性別：男

出生年月日：民國 73 年 01 月 23 日

住址：高雄市左營區文自路147巷39號

學歷：

國立中山大學物理系學士	(91.9-95.6)
國立交通大學光電工程學系顯示科技研究所碩士	(95.9-97.6)

碩士論文題目:

低溫鈍化技術於多功能薄膜之研究與應用

Application of low temperature passivation for muti-funtional thin film